University of New Mexico
UNM Digital Repository

Electrical and Computer Engineering ETDs | Engineering ETDs

6-26-2015

Design and Implementation of a Pivot Shift Prototype for Quantitative Analysis

Marco Antonio Espinoza Sanchez

Follow this and additional works at: https://digitalrepository.unm.edu/ece_etds

Recommended Citation
Espinoza Sanchez, Marco Antonio. "Design and Implementation of a Pivot Shift Prototype for Quantitative Analysis." (2015).
https://digitalrepository.unm.edu/ece_etds/81

This Thesis is brought to you for free and open access by the Engineering ETDs at UNM Digital Repository. It has been accepted for inclusion in Electrical and Computer Engineering ETDs by an authorized administrator of UNM Digital Repository. For more information, please contact disc@unm.edu.

Marco Antonio Espinoza Sanchez

Candidate

Electric and Computer Engineering

Department

This thesis is approved, and it is acceptable in quality and form for publication:

Approved by the Thesis Committee:

Wei Wennie Shu , Chairperson

Thomas P. Caudell

Marios S. Pattichis

Design & Implementation of a Pivot Shift Prototype for Quantitative Analysis

by

Marco Antonio Espinoza Sanchez

B.S., Chihuahua Institute of Technology, 2011

THESIS

Submitted in Partial Fulfillment of the

Requirements for the Degree of

Master of Science

Computer Engineering

The University of New Mexico

Albuquerque, New Mexico

May, 2015

©2015, Marco Antonio Espinoza Sanchez

Dedication

To my family and friends which always supported me through the University years.
I probably wouldn't be writing this thesis without their help.

Acknowledgments

I would like to thank and sincerely acknowledge my Thesis advisor Dr. Wei Wennie Shu for the guidance and support provided during the realization of this work. I would also like to thank Dr. Thomas P. Caudell and Dr. Marios S. Pattichis for being part of the thesis evaluation committee.

As well I would like to express my gratitude to *CONACYT (Consejo Nacional de Ciencia y Tecnología)* for all the support to make this happen.

Special thanks to my friend Engineer Jose Díaz for the help with the design and support of the prototype and to the medical staff leaded by Edmundo Berumen M.D. and Carlos Vega M.D. collaborating on the patient trials.

Design & Implementation of a Pivot Shift Prototype for Quantitative Analysis

by

Marco Antonio Espinoza Sanchez

B.S., Chihuahua Institute of Technology, 2011

M.S., Computer Engineering, University of New Mexico, 2015

Abstract

This thesis presents the utilization of a portable medical device intended to help in the diagnosis of the Anterior Cruciate Ligament(ACL) knee injury. The prototype consists of an embedded system integrated with various sensors including accelerometers and gyroscopes to provide force, orientation, and acceleration measurement. The prototype has been used to quantify the results of a medical test called pivot shift which tests the dynamic stability of the patient's knee. With the initial prototype built, limited clinical trials were conducted. Two schemes (metric based classification and k nearest neighbors) have been applied to the data set to empirically learn and judge ACL diagnosis.

Contents

List of Figures

List of Tables

Chapter 1

Introduction

This Thesis is based on the implementation of a previously design pivot shift prototype and its tests results in patients trails. The project consisted of an interdisciplinary collaboration between engineering and medical professionals.

The patient trials took place in Chihuahua, Mexico with collaboration of Edmundo Berumen M.D. and Carlos Vega M.D. at the Christus Muguerza del Parque Hospital between May 2013 and May 2014.

1.1 How the project got started

Part of the work showed in this Thesis backs from early 2013 before my arrival to UNM. Everything started with a call from a friend MD. Carlos Vega, that at that moment was working on some orthopedical research with regards of the ACL (anterior cruciate ligament) knee injury. In that call he mentioned got an idea of an electronics project that i may could possibly be interested in. He started talking about how he was working on this routine test called *pivot shift* and the problems it had with the equipment that he was using to measure the results. Then he finally

said "*could be a way to measure the movement or the force used during the test??, something to see the results on a PC..*". After that I contacted my friend also an electronics engineer Jose Diaz, got together, bought some microcontrollers and sensors and started playing with the project.

1.2 The ACL Injury

Knee injuries comprise about 55% of all sports injuries. Out of those, ACL (anterior cruciate ligament) tear represents one of the most common ones. Athletes involved in high demand disciplines like basketball, soccer, and football are more likely to develop this injury.

Briefly analyzing the knee anatomy the main three bones being part of the knee:

- Femur
- Patella
- Tibia

These bones connect to each other by ligaments to keep knee stability and protection limiting the movement. These ligaments can be described as:

- Collateral ligament. These ligaments can be found on the sides of the knees. The lateral collateral is located on the outside while the medial collateral on the inside. Their function consist on controlling the knee sideways motion and prevent unusual movement.
- Cruciate ligaments. Ligaments that are found inside the knee joint. The posterior cruciate ligament being located on the back while the anterior posterior

lies on the frontal part of the knee. They are responsible of the back and forth dynamic of the knee.

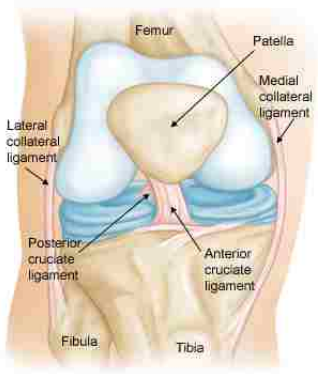

Figure 1.1: Normal knee anatomy, front view

Figure 1.1 shows the anatomy of a healthy knee where it can be seen how the ACL runs in the middle of the knee in diagonal direction, because of this prevents the tibia from sliding or moving out in front of the femur [1].

In the other hand figure 1.2 exposes a knee with the ACL injury, which among other things can be caused by:

- Direct impact or collision on one side of the knee
- Sudden stop of movement
- Overextend the knee joint
- Quick stop of motion and change direction while turning, landing from a jump or running.
- Slowing down while running
- Landing from a jump incorrectly

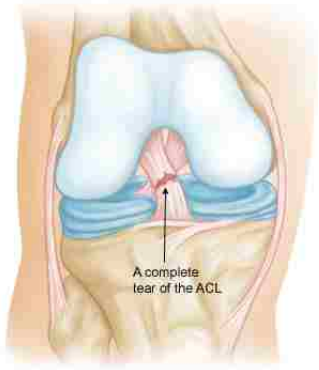

Figure 1.2: Frontal view of a knee with ACL injury

1.3 Diagnosis

Once there is the suspicion of an ACL tear, Doctors often use several techniques to determine if in fact an injury exist. There are invasive techniques like the knee arthroscopy and multiple non-invasive that can identified in two main groups, one being imaging tests like Radiography, CT scans and MRI, and the ones called routine tests or medical assessments including lachman, pivot shift and drawer tests.

1.3.1 Knee Arthroscopy

Knee arthroscopy is a minimally invasive technique that allows orthopedic surgeons to assess and treat several conditions affecting the knee joint. The procedure consist of a small incision in the vicinity of the affected joint. Then a tiny camera (around size of a pencil) is inserted along with fiber optics to provide light source. The camera transmits the images in real time to a monitor in the operating room, this way the specialist can gain multiple views of the joint area.

The surgeon can use this technique to assess, repair or remove damaged tissue, to do so, other small surgical equipment is inserted via a secondary incision around

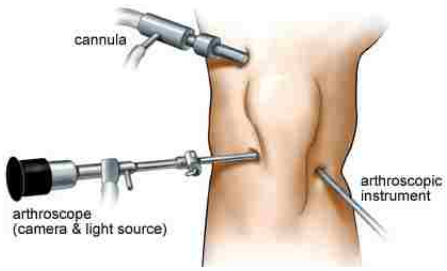

Figure 1.3: Arthroscopy equipment and setup on patient's knee

the knee. Aside from the invasive nature of this technique, it is the most effective one to determine the existence and severity of an ACL injury.

1.3.2 Non-Invasive Techniques

This section describes the routine tests and imaging techniques used in the diagnosis of the ACL injury, all of the following are considered non-invasive tests.

Computer Tomography

Commonly known as CT or CT scans. During the test, the scanner sends X-ray pulses to the patient's body. These pulses act during less than a second taking pictures of a thin slice of the area or organ of interest. In some cases the scanner is able to tilt its position allowing three dimensional CT.

This kind of scans are typically used to study an organ but can be used to examine blood vessels, bones, and the spinal cord.

In order to make the image analysis easier, an iodine dye (constrast material) is used to provide more clear pictures on the organs or area of study. This dye can be put in a vein (IV) or can be orally administrated.

CT can be used to visualize the ACL, however its visibility is not the best when haemarthrosis (bleeding into joint spaces) is present, situation where MRI has more significant results. Therefore, CT scan is used in cases when the patient cannot be exposed to an MRI, for example when the patient has a peacemaker, brain aneurysm clip or cochlear implant (ear implant).

Magnetic Resonance Imaging

Magnetic Resonance Imaging (MRI) is a medical imaging technique used in radiology to help physicians diagnose and treat medical conditions. One of the highlights of this technique is its non-invasive nature in the sense that no ionizing radiation (x-rays) is used. Instead, MRI makes use of powerful magnetic field and radio frequency pulses to produce pictures of tissues, organs and bones.

Protons (hydrogen atoms) in tissues containing water molecules are used to create a signal that after being processed forms an image of the body. Energy from the magnetic field at a certain resonant frequency is applied to the patient. Then, the excited protons emit a radio frequency signal that is measured by a receiver coil. This radio signals can be used to encode position information by changing the magnetic field using gradient coils. The contrast between different tissues is determined by the rate at which the excited atoms go back to an equilibrium state. Similarly to the CT scan, contrast agents may be used to provide better image results.

MRI results in better quality images of soft tissues like the ACL, having a high rate on ACL tear diagnosis with accuracy, sensitivity and specificity of more than 90%[2]. As well, MRI is also best for detecting concomitant mensiceal, ligamentous or chondral injuries[3].

Figure 1.4: MRI: Acute anterior ligament tear

KT-1000

This test developed by Dale Daniel, MD, back in the 1980's has been widely used over the years for the diagnose and follow up on patients with the ACL injury. This arthrometer is an objective instrument for the ACL reconstruction, which measures the anterior tibial translation in relation to the femur[4] between 20 and 30 degrees of knee flexion.

To perform the test, the KT-1000 is firmly attached to the patient's leg by two bands, after this the arthrometer is pulled to the tibia to provide an anterior force. Audible feedback (beeping) to the examiner is noticed at 15, 20 and 30 pounds of applied force. The output of the test consist on the tibia translation with respect to the femur in millimeters (mm). With this data, the laxity (how loose the ligament is) is calculated in side-to-side difference between the patient knees.

From extensive testing, the literature states that an intact or partial ACL tear

Figure 1.5: KT-1000 test measuring anterior-posterior knee translation

have less than 3 mm of increased anterior translation during the test[4].

Lachman test

The Lachman test named after orthopedic surgeon John Lachman , is a noninvasive medical test performed for the diagnose of the ACL injury known for its high accuracy. In order to make the test, the examiner ensures the tibia with one hand while securing the femur with the other one. The knee, is flexed at 30° while the patient lies supine. The examiner stabilizes the femur and applies force in anterior direction on the tibia. While a healthy ACL should prevent forward translational movement, a positive result for an ACL injury will be a noticeable anterior translation of the tibia. Depending on the anterior translation registered its laxity is defined as: grade I for 1 mm-5 mm, grade II for 6 mm-10 mm and grade III for anterior translation over 10 mm.

This test can be complemented with the use of the KT-1000 in order to determine the anterior translation in millimeters[5].

(a) Lachman test

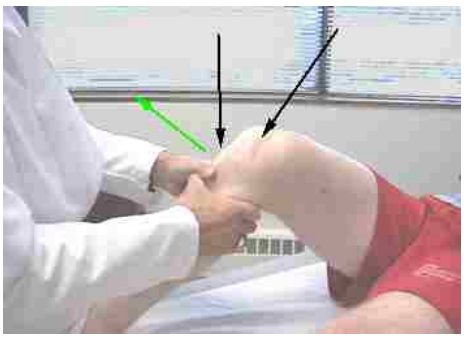

(b) Drawer test

Figure 1.6: Clinical assessments for the ACL diagnosis

Drawer test

The drawer test is a clinical test used in the initial evaluation when there is suspicion of an ACL tear injury. Similarly to the Lachman test the patient stands with the hips flexed 45° and knees flexed to 90° with the feet flat on the table. With the knee flexed verification of the relaxation is done by hamstring palpation, this is done in order to prevent false negatives. The thumbs are placed along the joint line on both sides of the patellar tendon. After setup of the grip, an anterior force is then applied to the proximal tibial with gentle to and fro (back and forth) movement to assess for increased translation between knees. The test is considered to be positive if the tibia pulls in forward or backward direction more than normal.

Pivot Shift test

This test is the combination of internal rotation and valgus force applied to the leg which helps to determine the dynamic instability of the knee. The test is performed with the patient lying in supine position starting from the knee in full extension and then gently flexing to approximately 40° . A valgus torque and internal rotation are applied to the leg. A positive pivot shift test is defined as a forward subluxation

Figure 1.7: Pivot Shift test

of the tibia during the change of direction. This clinical test tries to reproduce the event when an ACL tear occurs, when the knee gives way due the loss of the ACL[6].

The pivot shift is a relatively complex test. For this reason and the lack of a quantitatively accepted method to measure the results[7], is evaluated only on the basis of the examiner's experience[8].

Still with this limitations the test is considered one of top three applied techniques towards the diagnosis of an ACL condition, part of this has to do with the fact that contrary to the Lachman and Drawer tests, the Pivot Shift is the only of the three that analyses the dynamic and rotational stability of the anterior cruciate ligament, which more accurately relates to the knee function.

The complexity of the test using rotational and valgus forces makes the quantitative analysis more challenging in comparison with uniplanar stress testing like the one present in the Lachman test that can be measured with the KT-1000.

For this reason, several studies[7, 9] have tried to decompose the pivot shift movement into quantifiable parameters suggesting:

- anterior posterior translation
- anterior posterior acceleration

- anterior posterior rotation

as valid metrics towards giving objective nature to the test results.

The work showed in this thesis represent the effort of the design and implementation of a portable electronic prototype capable of reproducing acceleration and rotational metrics out of the pivot shift. *"The ideal instrumented clinical examination test should be noninvasive, portable, and applicable in both operating room and office environments"*[9].

Chapter 2

The Pivot Shift Prototype: Hardware Design

This chapter describes in detail the hardware specifics of the previously designed prototype, including an overview of the microcontroller used, the sensors and their specifications as well as the communication that takes place between the embedded system and the PC.

2.1 Arduino

Arduino is an open source and open hardware computing platform based on simple input/output (board) and a development environment that is based on the Processing[10] programming language.

Hardware wise Arduino consist of a microcontroller with a set of peripherals like digital input/output pins, analog input pins (likely to be used when working with analog sensors), LED's for power and user feedback, and support for communication

protocols like Serial, I^2C[11], SPI and Bluetooth among others.

Arduino offers more than a dozen of different development boards varied in dimension, features and application. However they share the same programming language, which facilitates porting applications from one board to another. The board connects to a computer via USB and communicates using standard serial port and can run both standalone or connected to another device or computer.

Both the Arduino software and the boards itself are cross-platform running on Windows, Linux, and Mac OSX. This was a very important feature taken in consideration to choose this embedded solution [12].

The Arduino IDE provides the functionality of code editor, serial monitor, and lastly and more important it is used to translate the Arduino code which is based on Wiring (an open-source programming framework for microcontrollers) into C code, then handed over to the avr-gcc compiler that makes the final translation producing the program that gets flashed in the microcontroller. Besides the use of the Arduino programming language, extended functionality and low level programming can be achieved creating custom C/C++ libraries[13].

A thing worth mentioning is the big role the community plays on the success and continue development the Arduino platform, this due contributions in code and projects from enthusiasts and hobbyists alike.

2.1.1 Arduino Mini Pro 328

This board takes a small and minimal design of the Arduino which made it more suitable for the project. These are the main features of the board:

- Microcontroller Atmega328[14] at 8MHZ

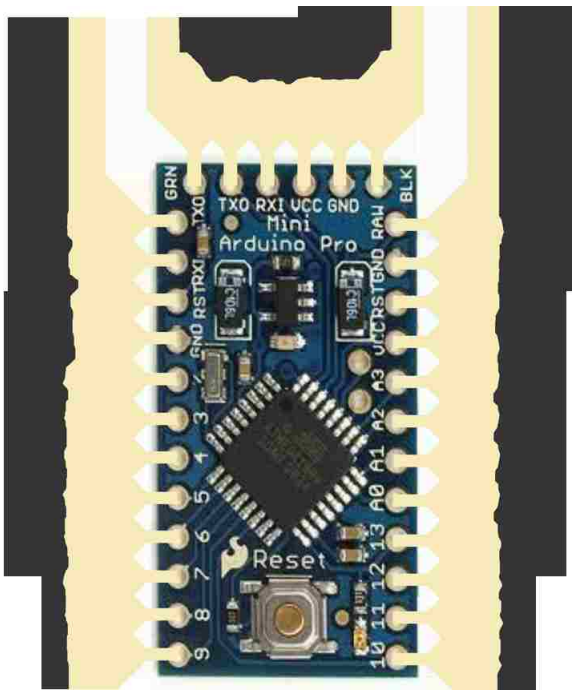

Figure 2.1: Arduino Mini Pro

- Low voltage board, 3.3V
- Thin PCB 0.8mm
- 3.3V regulator
- Max 150mA output
- DC input 3.3V up to 12V
- Power and Status LEDs
- Analog Pins: 8
- Digital I/Os: 14

The main and most important component is the Atmega328p microcontroller, which is a 8-bit AVR RISC-based microcontroller[15] that combines 32 KB ISP flash

memory, 2 KB SRAM, 1 KB EEPROM, 23 general purpose I/O lines, 32 general purpose working registers, internal and external interrupts support, three timers, a Serial programmable USART, SPI and IC^2 port, a 10 bit A/D converter. All with low power requirements from 2.7-5.5 volts.

2.2 MEMS:Accelerometer and Gyroscope

MEMS (Microelectromechanical systems) is a process technology to bundle together mechanical and electrical components in tiny integrated devices or systems. They are fabricated using integrated circuit (IC) batch techniques and can range in size from a few micrometers to millimeters.

MEMS increased their popularity in the last few years and now can be seen in multiple areas such as automotive, medical, electronic, communication, etc. Examples are:

- accelerometers for airbag sensors
- inkjet printer heads
- hard drives read/write heads
- microvalves
- blood pressure sensors
- log exercise activity on professional athletes[16]

Practically speaking a MEMS is a silicon chip which contains mechanical microstructures, microelectronics, microsensors and microactuators.

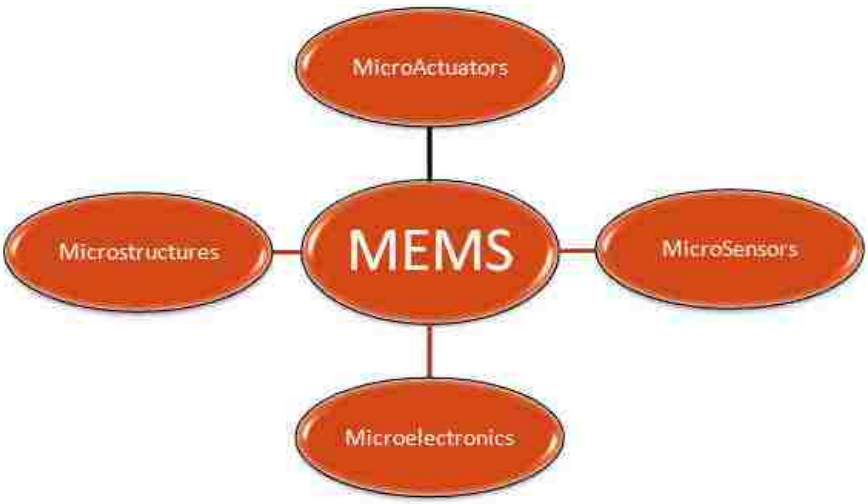

Figure 2.2: MEMS components diagram

The microsensors detect changes in the environment measuring mechanical, thermal, magnetic, chemical or electromagnetic information, while the microelectronics take this information to signal the microactuators in order to react and create changes to the environment.

Nowadays power management in portable electronics is a must to extend battery life, a good thing about MEMS sensors is that they can sense when a device is not being used and put it into sleep mode.

The following section describes the functionality and characteristics of the MEMS acceleromer and gyroscope used in this project.

2.2.1 Accelerometers

A MEMS accelerometer is different from a integrated circuits in the fact that a proof mass is machined into the silicon. Then when acceleration a is applied, the mass m displaces according to Newton's second law $F = ma$, which is detected by the sensor. This mass proof disturbs the capacitance of a nearby node; that change is

measured and then filtered.

One of the most important specifications to have in mind when looking for an accelerometer is the number of axes. MEMS proof mass can measure one parameter in each available axis, that being said a one axis accelerometer can sense the g force ($g = 9.8\frac{m}{s^2}$) in a single direction. Now is getting more common to use three-axis devices which returns the acceleration on X,Y,and Z directions.

The output of a three-axis accelerometer can be calculated as

$$a_m = \frac{1}{m}(F - F_g) \tag{2.1}$$

where a_m represents the acceleration, m the mass of the body, F the sum of all the forces actuating on the body (gravity included), F_g is the gravity force. As mentioned before, the accelerometer can be constructed attaching a proof mass to a spring. An upward or downward acceleration in the sensor causes the proof mass to displace, which can be measured to calculate the acceleration. This acceleration can be accounted to the term F in equation 2.1.

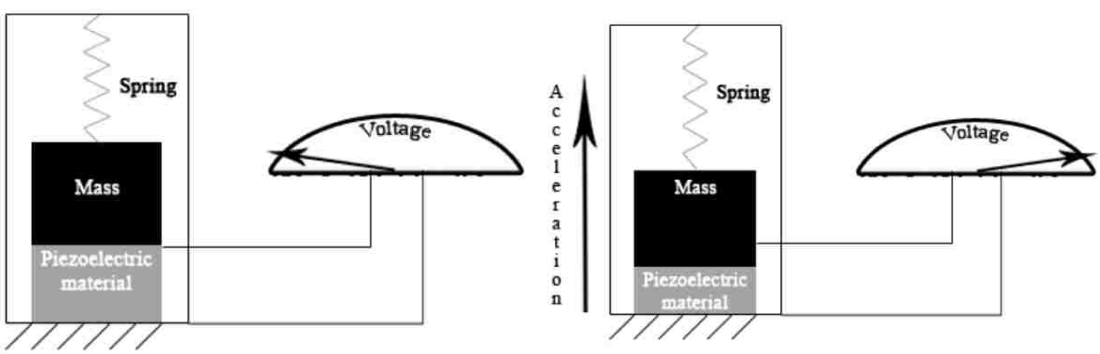

(a) (b)

Figure 2.3: Piezoelectric accelerometer, spring moves as acceleration forces act upon the sensor, producing a voltage proportional to that force

The second term F_g is part of the model of the accelerometer because the force of the gravity not only accelerates the sensor body, it also produces the displacement of the proof-mass. For example, if the accelerometer stays still in horizontal position on a table, is not accelerating and $F = 0$, but still gravity produces a downward deflection on the proof mass that appears equivalent to an upward acceleration of the sensor at 1g. Free fall shows a similar situation, in which $F = F_g$ and there is no displacement of the proof mass, therefore no acceleration is measured (output of the accelerometer is zero)despite the fact that the device is accelerating at 9.8 m/s due the gravity. This phenomenon is a consequence of the statement from Newton's law that the sum of the gravitational and inertial forces equals to zero on an body in free fall. From the previous we can conclude the following:

- when the accelerometer lies at rest it will output an $a = 1g$, due gravity.
- when the device is on free fall the acceleration outputs $a = 0$.

2.2.2 Gyroscope

A gyroscope is a device used to measure rotation and detect inertial angular motion. There are many kind of gyroscopes which can work based on different principles for example the mechanical kind of gyroscope that measures the Coriolis force applied to a body in a rotating frame. MEMS gyroscopes typically use vibrating structures because of the size constrain that makes difficult to incorporate micro-machined rotating parts with the required mass[17].

MEMS gyroscopes use the Coriolis effect. Taking as example figure 2.5, consider a mass moving in v direction. When an angular motion is applied (red arrow), the Coriolis effect makes the mass experience a force in the direction of the yellow arrow.

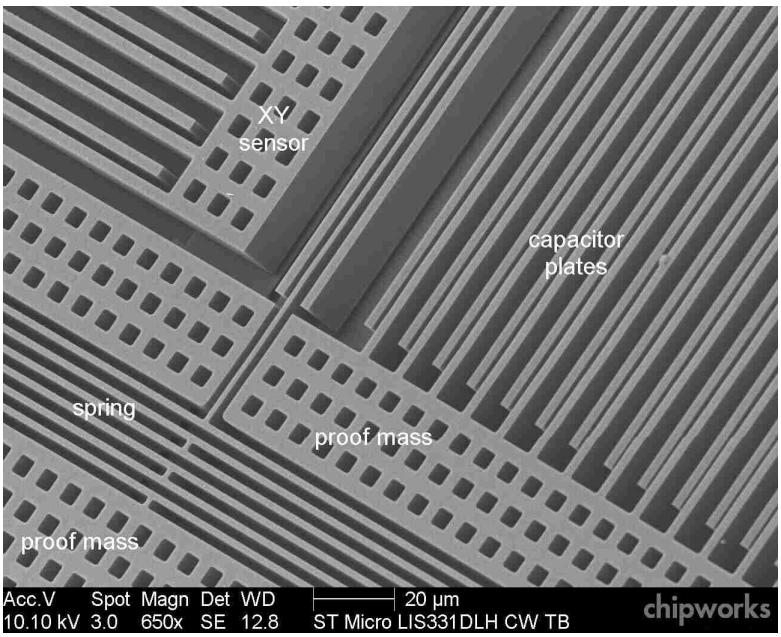

Figure 2.4: Three-Axis accelerometer LIS331DLHXY used in iPhone 4 in detail, micromachined proof mass interleaved with capacitive sensors

In this kind of gyroscope (MEMS) the resulting physical displacement is read using capacitive sensors.

These gyroscopes use a tuning fork configuration, in which two masses are placed side to side, they oscillate and move constantly in opposite directions. When angular motion is applied the Coriolis force on each mass acts in opposite direction. The difference between their capacitance is then measured to produce the rotation metric.

As counter example, when linear acceleration is applied to the two masses, both move towards the same direction, this produces a differential capacitance of zero, which makes the measurements of the gyroscopes not to be affected by acceleration forces.

Similarly to the accelerometers, MEMS gyroscopes can be found in single axis or three-axis presentations. Since they measure the angular rate or velocity the output

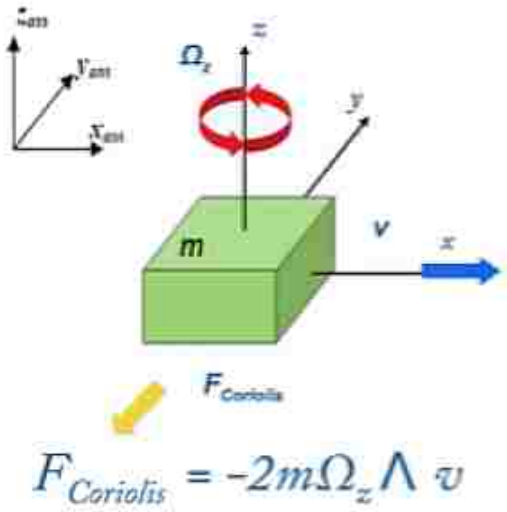

Figure 2.5: MEMS gyroscope submitted to Coriolis effect

unit is often dps (degrees per second), RPMs (revolutions per minute), and radians per second.

2.2.3 MMA7361LC: Three Axis Low-g Accelerometer

The MMA7361LC was the accelerometer used in the first pivot shift prototype and from which came many of the test results to be analyzed in following chapters. Since this is an analog device, the output signals are voltages proportional to the measured acceleration. The main features of the device are:

- selectable sensitivity $\pm 1.5g, \pm 6g$
- acceleration sensing for X, Y and Z axis
- 2.2 to 5 supply voltage range
- low current consumption 400uA

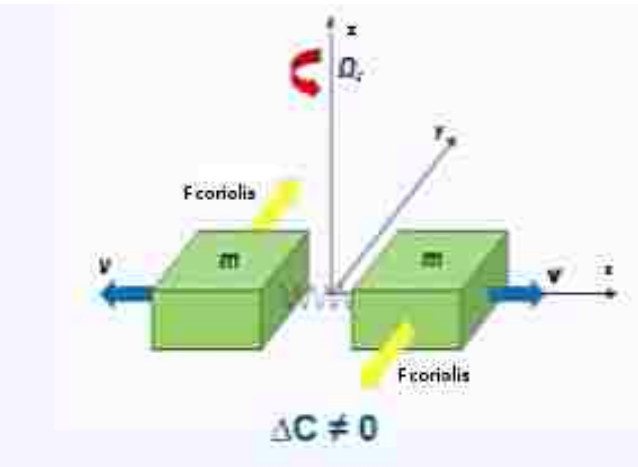

Figure 2.6: MEMS gyroscope submitted to angular motion

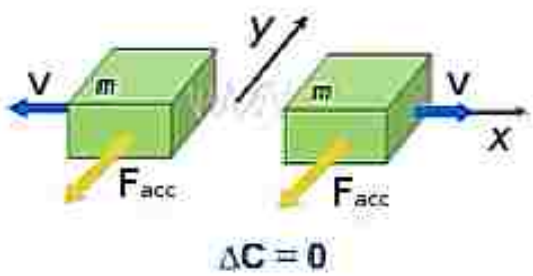

Figure 2.7: MEMS gyroscope submitted to linear acceleration

- 800 mV/g sensitivity at $\pm 1.5g$ range
- low cost

The interaction between the accelerometer and the Arduino is as follows. The accelerometer is powered up to 3.3 volts provided by the Arduino (therefore reference voltage is 3.3v). Out of the box the MMA7361LC works on sleep mode reducing the operating current to 3uA, which is great for power saving purposes but turns off the output signals. In order to disable sleep mode and turn on the x, y, and z outputs sleep mode pin (#7) should be set high, which was achieved using a pull up resistor.

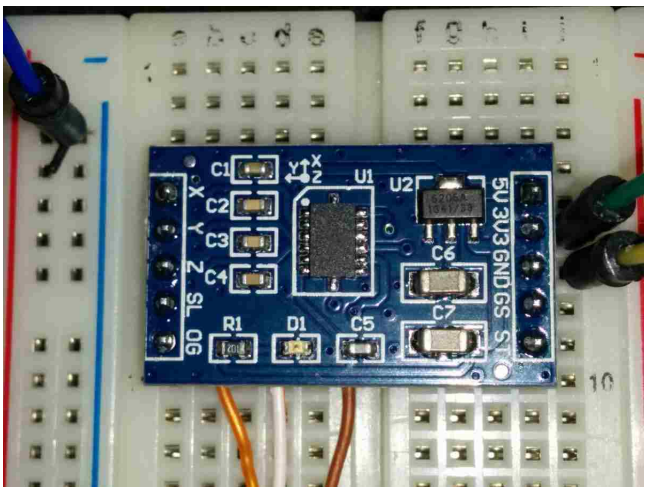

Figure 2.8: MMA7361LC analog accelerometer breakout board showing respective directions for each axis

The three axis outputs are then connected to analog inputs in the Arduino denoted by A0, A1, and A2 pins. Capacitors are connected to the outputs to minimize clock noise and on VDD to decouple the power source.

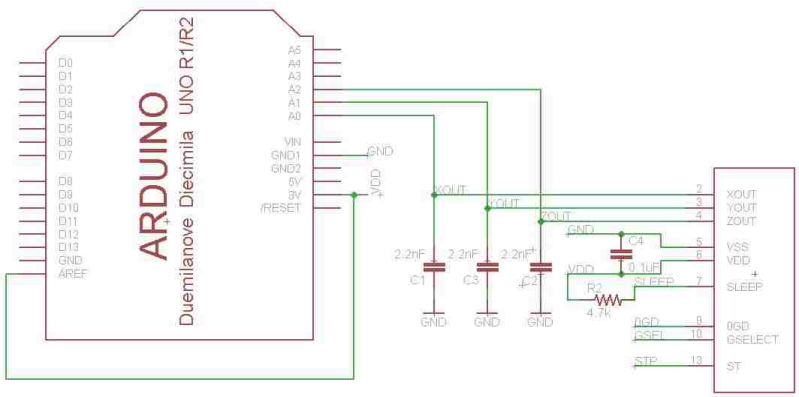

Figure 2.9: MMA7361LC and Arduino connection diagram

The Arduino reads these analog voltages from the accelerometer and then digitalizes them using the internal analog to digital converter. In this model the analog to

digital converter has a 10 bit resolution which means that it will map input voltages from 0 to 3.3 volts into integer values between 0 to 1023 ($2^{10} - 1$). This gives a resolution of 3.3V/1024 or 3.2mV between readings. The maximum number of samples that can be read in a second is 10,000, it takes about 100 microseconds to read an analog input.

The device can measure both positive and negative acceleration (depending on the direction of the force being applied). With no acceleration the output should be at midsupply. For positive acceleration the output voltage will increase above $V_{DD}/2$ as for negative will go decrease below $V_{DD}/2$.

The following is a simpe Arduino code to read the three outputs from the accelerometer and print the values via the serial port [18].

```
1
2  /* MMA7631 ANALOG 3axis accelerometer test*/
3  char breaktrans;
4  float valx,valy,valz;
5  void setup()
6  {
7    while (!Serial);
8    Serial.begin(19200);
9    Serial.println("Send a 1 to start transmission)");
10   while (Serial.available() <= 0) {}        //waiting for some
       string..
11   breaktrans='1';                            // to start the
      test
12 }
13 void loop()
14 {
15   breaktrans=Serial.read();
16   if(breaktrans=='1'){        //read data from sensor
17     while(1){
18      breaktrans=Serial.read();    //to be able to stop
19      valx=analogRead(A0);
20      valy=analogRead(A1);
21      valz=analogRead(A2);
22
23       Serial.print("x "); Serial.println(valx);
```

```
24        Serial.print("y "); Serial.println(valy);
27        Serial.print("z "); Serial.println(valz);
28        if(breaktrans=='0'){break;}    // stop transmission
29      }
30    }
31  }
```

This code (sketch) initializes the serial port at a baud rate of 19200bps then in order to start the transmission the Arduino waits until receiving a string '1' (can come from another embedded system or computer connected to the device). Transmission is ended after receiving a string equal to '0'. This pairing routine to start and end transmission is important when the system is designed to run on battery. The *analogRead*() function takes care of the ADC sampling of the pins used as analog inputs, in this case the constants A0, A1 and A2 mapped to pins 23, 24 and 25 of the Atmega328.

After uploading the code to the Arduino board we can see how the voltages are received and coded to integer values between 0 and 1023 (due the 10 bit analog to digital converter).

Looking at figure 2.14b it's clear how the output registered by the z axis (blue) presents an offset from the other two axis. This difference represents the gravitational force being applied to that axis. Conversely if the device is rotated 90 degrees horizontally and vertically then the gravitational force will be spotted acting on the x and y axis.

Once the system is able to get and perform the quantization of the accelerometer outputs, two things are helpful to give some context to the data obtained. The first thing to is to convert the raw value returned by the ADC (analog to digital converter) to Volts. To do so we do:

$$ADC_{Voltage} = Raw_{ADC} * Vref/1023 \tag{2.2}$$

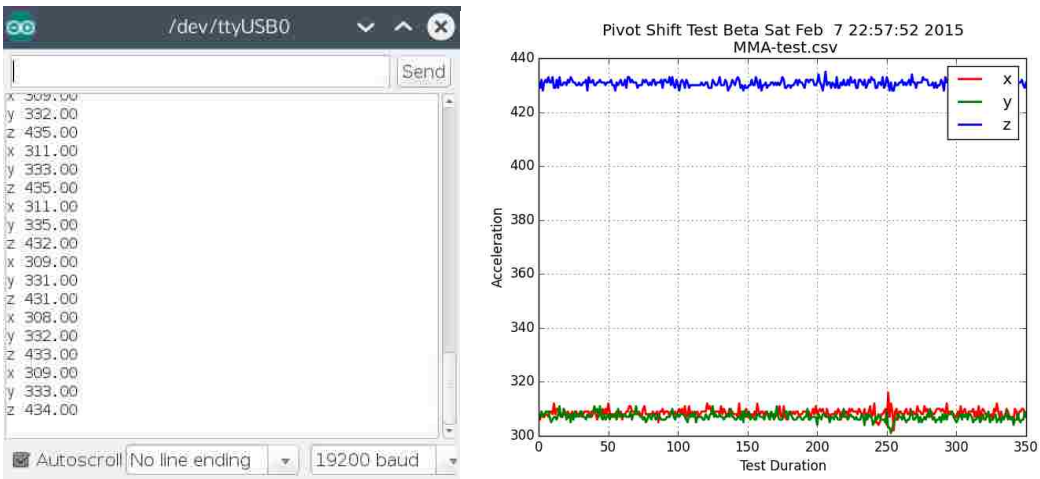

(a) Arduino IDE serial port monitor

(b) Output for x, y and z axis

Figure 2.10: Reading the output of the MMA7361LC accelerometer resting at horizontal position

Where Raw_{ADC} is the integer from 0 to 1023 got from the ADC, $Vref$ is the reference voltage in this case 3.3V and the 1023 representing the levels of quantification or discrete values the ADC can provide.

After this, the Zero-g voltage is subtracted from the $ADC_{Voltage}$. The Zero-g voltage is the voltage that each of the axis outputs when no acceleration ($0g$ acceleration) is being applied. This is typically provided in the device data-sheet although is easy (and recommended) to calculate practically because can vary from chip to chip.

	Data-Sheet	From device testing
Xout	1.65 V	1.591 V
Yout	1.65 V	1.705 V
Zout	2.45 V	2.205 V

Table 2.1: Zero-g voltage taken from data-sheet and device testing

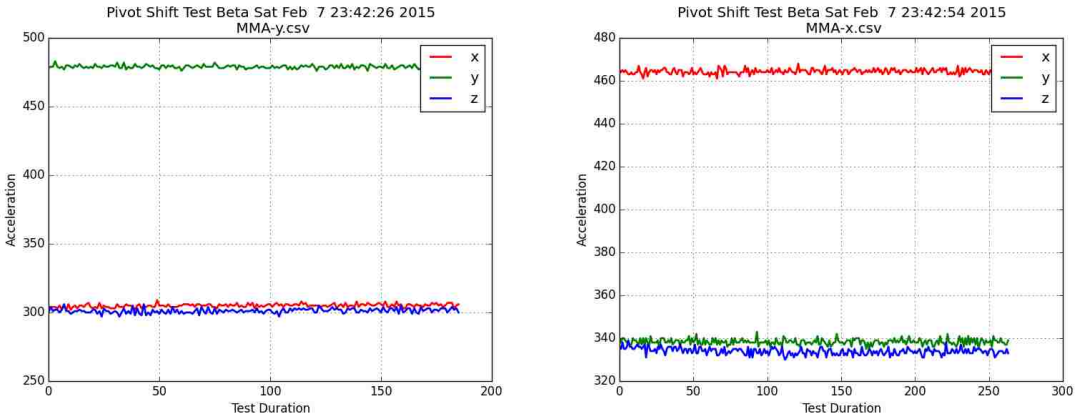

(a) Gravity acting on Y axis (b) Gravity acting on X axis

Figure 2.11: The effect of gravity on accelerometer readings

From the table above it can be seen a slight difference between the typical values provided from the data-sheet and the actual values got from testing the device.

Now finally to go from Volts to G's ($1g = 9.8m/s^2$) the following calculation is performed for each of the axis

$$\begin{aligned} G_x &= (ADC_{XVoltage} - Zero_X)/sensitivity \\ G_y &= (ADC_{YVoltage} - Zero_Y)/sensitivity \\ G_z &= (ADC_{ZVoltage} - Zero_Z)/sensitivity \end{aligned} \tag{2.3}$$

where $Zero_X$, $Zero_Y$, and $Zero_Z$ are 1.59V, 1.705V and 2.205V respectively (from table 2.1). The sensitivity value comes directly from the device specifications which can be 800mv/g or 206 mv/g for $\pm 1.5g$ and $\pm 6g$ operation ranges, which in this case is set to operate at $\pm 1.5g$.

2.2.4 LSM9DS0: 3D Accelerometer/Gyroscope module

The LSM9DS0 is a system in package featuring a three-axis accelerometer, gyroscope and magnetometer also known as a nine degrees of freedom device (9DOF). Each of the three sensors in the device supports programmable operating ranges. The accelerometer has a full scale of $\pm 2g/\pm 4g/\pm 8g/\pm 16$ g, the gyroscope an angular rate of $\pm 245/\pm 500/\pm 2000$ dps (degrees per second) and the magnetometer a magnetic field of $\pm 2/\pm 4/\pm 8/\pm 12$ gauss. The device includes an I^2C serial bus supporting standard and fast mode (100 kHz and 400 kHz) and an SPI serial interface.

Accelerometer and Gryoscope characteristics are found in the following tables:

Parameter	Test conditions	Specification	Unit
Linear acceleration measurement range		±2	g
		±4	
		±6	
		±8	
		±16	
Linear acceleration sensitivity	Linear acceleration=±2	0.061	mg/LSB
	Linear acceleration=±4	0.122	
	Linear acceleration=±6	0.183	
	Linear acceleration=±8	0.244	
	Linear acceleration=±16	0.732	
Linear acceleration sensitivity change vs. temperature	From -40 °C to +85 °C	±1.5	%
Linear acceleration typical zero-g level offset accuracy		±60	mg
Operating temperature range		−40 to +85	°C

Table 2.2: LSM9DS0 Accelerometer characteristics

Before continuing, lets define some of the terminology showed on the previous tables. When talking about sensors it is common to see terms like range, sensitivity and zero levels.

Parameter	Test conditions	Specification	Unit
Angular rate measurement range		±245	dps
		±500	
		±2000	
Angular rate sensitivity	Angular rate=±245	8.75	mdps/digit
	Angular rate=±500	17.50	
	Angular rate=±2000	70	
Angular rate sensitivity change vs. temperature	From -40 ° C to +85 ° C	±2	%
Angular rate typical zero-rate level	245 dps	±10	dps
	500 dps	±15	
	500 dps	±25	

Table 2.3: LSM9DS0 Gyroscope characteristics

The range represents the levels the sensor's output signal can achieve (maximum and minimum values), that in regards of the accelerometer is expressed in $\pm g$, with option of five different ranges to choose from. For instance, if the accelerometer is working in the $\pm 2g$ range, this means that if a 4g force is applied it will not be properly displayed by the output since the maximum is set to 2g. For this reason is important to know the application in which the device will be used on, to select the appropriate output range. From the previous statement would be very tempting to say that the best solution is to select the broadest range, however this is were the sensitivity comes into play.

The sensitivity is the ratio of change between the input and output signal in the sensor. The metric is specified at a particular operating voltage typically in mV/unit for analog devices and LSB/unit or unit/LSB for digital output devices. For the accelerometer it's seen in mg/LSB, where LSB stands for least significant bit. LSB relates to accuracy of the digital representation of the measured unit, in this case acceleration. For example from table 2.2 we see that when using range $\pm 2g$ there is a sensitivity equal to $0.061mg/LSB$, this means that when the lowest order bit in the output changes, the acceleration had a change of 0.061mg's or $0.0005978m/s^2$,

in other words $0.0005978 m/s^2$ is the tinniest change in acceleration the sensor can have between readings. Looking at the specification can be seen how for a broader range the sensitivity value increments as well, which makes the sensor less accurate.

Additional to the convenience of providing both acceleration and gyroscope metrics in the same chip, the LSM9DS0 output signals deliver digital data in useful units like G's and dps for acceleration and angular velocity respectively. That being said, when interfacing with digital sensors like the LSM9DS0 there is no longer need of using the analog to digital converter of the Arduino board, removing some overhead of reading and sampling the analog inputs, as well as making the conversion of ADC units to Voltage and then G's as seen previously using the MMA7361LC accelerometer.

Other fact worth mention is that the digital sensor eases the scalability of the system, e.g when using the MMA7361 three input lines are required to communicate the device with the Arduino. Now, if we were to implement a second accelerometer or gyroscope in the system, three additional lines would be required (X_{out}, Y_{out}, Z_{out}), which equals the maximum number of analog inputs for the Atmega328 microcontroller that supports up to 6 (without multiplexing[19]). In the other hand, to communicate two LSM9DS0's with the Arduino (2 accelerometers and 2 gyroscopes) via I^2C requires only two lines as the following section will show.

2.2.5 I²C Protocol

From the two protocols offered by the LSM9DS0 I²C was the one used to communicate the accelerometer to the Arduino board.

The I²C protocol requires two wires to connect a single master to a slave, unlike SPI that requires four lines to achieve the same. I²C supports multi-master system that allows more than one master to communicate with all slaves in the bus. I²C

Term	Description
Transmitter	The device which sends data to the bus
Receiver	The device which receives data from the bus
Master	The device that initiates a transfer, generates clock signals and terminates transfers
Slave	Device addressed by the master

Table 2.4: I^2C terminology

supports two main data rates called normal and fast mode running at 100kHz and 400 kHz respectively.

There are two signals associated with the I^2C bus: the serial clock line (SCL) and serial data line (SDA). The SDA line is a bidirectional line that can be used for sending and receiving data both by master and slave devices. These lines use pull-up resistors to keep a high state when the bus is free.

The bus drivers are "open drain", which means that they can pull the signal line to a low state, but cannot turn it to high. This implementation prevents potential damage to the drivers and excessive power dissipation, disables what is known as bus contention where a device tries to drive the line high while other tries to pull it low.

Bus operation

The operation on the bus starts when the master performs a start condition, which is defined as a high to low transition on SDA (data line) while SCL (clock line) is high, at this point the bus is considered busy. The next byte of data contains the address of the slave in the first 7 bits, the 8th bit determines whether the device is transmitting or receiving from the slave, while a 9th bit is used as NACK/ACK bit. When this address is sent, then all devices compare it with their own to check if they

are being addressed by the master.

Acknowledge is mandatory for this protocol, both for the data and address frames. Once the first 8 bits (address and r/w) are sent, the receiving device is given control over the SDA line. To successfully generate the acknowledge, the receiver needs to pull low the SDA line prior the 9th clock pulse.

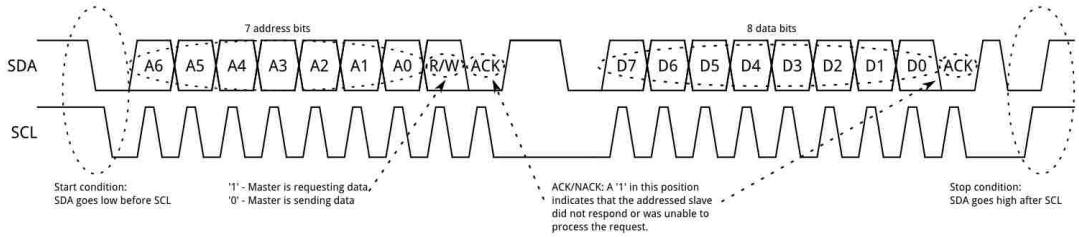

Figure 2.12: I^2C signals, showing the start condition, address and data frames, ,and stop condition

Data transmission can start after the address frame has been sent. During data transmission the master continues the with the control and generation of the clock pulses while the data is placed in SDA line by the master or the slave, depending the value of the r/w bit (8th bit of address frame). The number of data frames is arbitrary, and most slaves will auto-increment the internal registers to allow subsequent reads or writes.

The operation of the protocol end with a stop condition defined by a low to high transition on the data line SDA while the clock line stays high.

2.2.6 Getting data from the LSM9DS0

This section shows the required connections to be made between the LSM9DS0 and the Arduino board in order to communicate. The following schematic shows a configuration of two LSM9DS0 connected to the Arduino Mini board using the

previously introduced I^2C communication protocol.

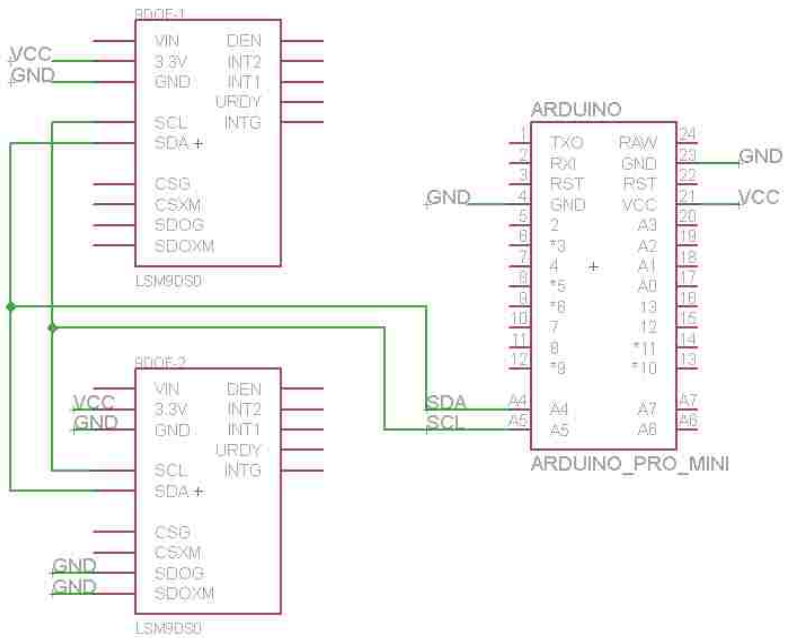

Figure 2.13: Schematic diagram of two LSM9DS0's connected to an Arduino Mini board under I^2C

Compared to the connection of the MMA7361 back in figure 2.9 this one looks pretty straightforward considering that includes two LSM9DS0 modules. In this configuration the Arduino acts as master for the I^2C leaving the LSM9DS0's as slaves.

The two LSM9DS0 boards share the bus for the clock and data signals SCL and SDA. The clock signal is controlled and generated by the Arduino while the SDA can be used to send and receive data from the accelerometers. Initially both LSM9DS0 boards have the same address which makes impossible to the master to differentiate from each other. To solve this, the least significant bit of the address of one of the modules is changed by setting pins SDOG and SDOXM to a low state. Arduino board and inertial modules are powered up by 3.3 Volts.

The next code snippet shows the Arduino data adquisition from the LSM9DS0 inertial module.

```
#include <Wire.h>
#include <Adafruit_LSM9DS0.h>
#include <Adafruit_Sensor.h>
/*
 *  i2c arduino pins
 *  Arduino analog input 5 - I2C SCL
 *  Arduino analog input 4 - I2C SDA
 */
Adafruit_LSM9DS0 lsm = Adafruit_LSM9DS0();
char breaktrans;
void setupSensor()
{
  // 1.) Set the accelerometer range
  lsm.setupAccel(lsm.LSM9DS0_ACCELRANGE_2G);
  // 2.) Setup the gyroscope
  lsm.setupGyro(lsm.LSM9DS0_GYROSCALE_245DPS);
}

void setup()
{
  while (!Serial);
  Serial.begin(19200);
  Serial.println("Send a 1 to start the test");
  while (Serial.available() <= 0) {}        //waiting for some
    string..
  breaktrans='1';                            // to start the
   test
  // Try to initialise the device
  if (!lsm.begin())
  {
    Serial.println("Unable to initialize the LSM9DS0. Check
     your wiring!");
    while (1);
  }
  Serial.println("Found LSM9DS0 9DOF");
  Serial.println("");
}

void loop()
{
```

```
38    breaktrans=Serial.read();
41    if(breaktrans=='1'){          //read data from sensor
42        while(1){
43        breaktrans=Serial.read();   //continue to read to catch
           stop condition
44        //getting the sensor event
45        sensors_event_t accel, mag, gyro, temp;       //from
           adafruit sensor master library
46        lsm.getEvent(&accel, &mag, &gyro, &temp)
47        //reading the accelerometer
48        Serial.print("accelx "); Serial.println(accel.
           acceleration.x);
49        Serial.print("accely "); Serial.println(accel.
           acceleration.y);
50        Serial.print("accelz "); Serial.println(accel.
           acceleration.z);
51        //reading the gyroscope
52        Serial.print("gyrox "); Serial.println(gyro.gyro.x);
53        Serial.print("gyroy "); Serial.println(gyro.gyro.y);
54        Serial.print("gyroz "); Serial.println(gyro.gyro.z);
55        if(breaktrans=='0'){break;}   // stop transmission
56      }
57    }
58  }
```

This code provides the same functionality shown in the program for the MMA7361 with the difference of addition of angular velocity provided by the gyroscope. Two main libraries are imported, Wire which allows communication with I^2C/TWI devices, and the Adafruit library[20] that incorporates the class Adafruit_LSM9DS0 that includes useful functions to easily configure the device to the different ranges as well to get the outputs from each of the axis and sensors available (accelerometer, gyroscope and magnetometer) without coding to a register level.

The function *setupAccel* lets you choose the range of operation for the accelerometer from the following options

- LSM9DS0_ACCELRANGE_2G

- LSM9DS0_ACCELRANGE_4G
- LSM9DS0_ACCELRANGE_8G
- LSM9DS0_ACCELRANGE_16G

whereas *setupGyro* allows setting the angular velocity range to

- LSM9DS0_GYROSCALE_245DPS
- LSM9DS0_GYROSCALE_500DPS
- LSM9DS0_GYROSCALE_2000DPS

sensor_event_t is a structure that provides a single sensor events in a common format. In this way each sensor creates its own object from which it can retrieve its respective data from. Calling *getEvent* grabs sensors new data, so in order to continuously get new readings it needs to be executed recursively.

Similarly to the test done with the analog accelerometer, these are the results of flashing the Arduino board with the previous code and getting some data from the sensor.

As expected the graph of the three axis acceleration at rest (horizontal postition) is pretty similar of what was presented on 2.14b with the difference that in this case the outputs are in g's already.

With the goal of comparing the sampling rate between each of the chips, previous Arduino programs were slightly modified to transmit data during a period of 10 seconds. In the results the MMA7361C delivered an average of 165 triplets (Xout, Yout, Zout) as the LSM9DS0 delivered an average of 650 triplets. This difference is caused in some proportion to the overhead caused by reading the analog inputs and performing the analog to digital conversion when using analog sensors. When

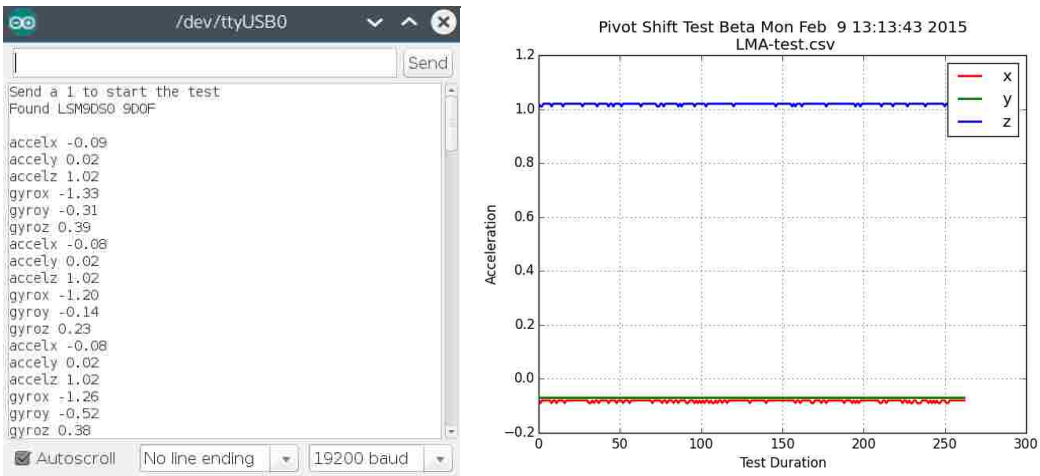

(a) Arduino IDE serial port monitor

(b) Output for x, y and z axis

Figure 2.14: Reading the output of the LSM9DS0 accelerometer resting at horizontal position

performing the same test but adding the angular velocity readings from the gyro the results were an average of 290 samples for each variable.

2.3 The Prototype

This section describes the idea behind the pivot shift tester prototype and how it was implemented. Going back to what was introduced in the first chapter we saw the different medical tests and tools commonly used in the diagnose of the injury of the anterior posterior ligament. We were able to identify them in two main groups:

- imaging techniques
- routine tests

The problem with the first group (imaging) resides in the fact that uses equipment considerably expensive, in such a way that the patient often needs to visit a clinic or

hospital to take test. It is highly unlikely to find them in the specialist's office and both CT scans and MRI typically have a cost superior to $1000 US dollars. Aside from the economic factor, other disadvantage that the imaging techniques have is that both tests the patient's leg and knee in a static environment, reason why in some cases is difficult to assess a definitive diagnose if the information provided by the image is not completely evident.

Here we provide an example, the first image (MRI) shows a complete tear of the ACL ligament. In an image like this the specialist is able to confirm the ACL injury without much hesitation, because the ligament simply is not there anymore.

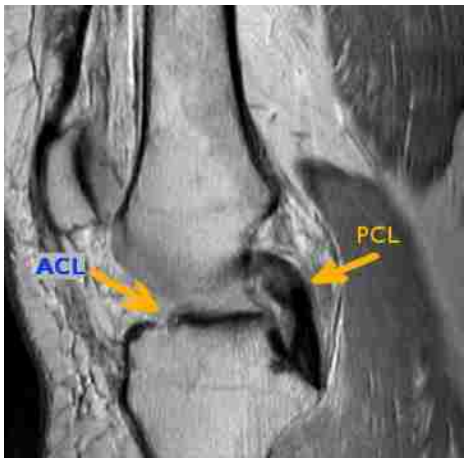

Figure 2.15: MRI, complete tear of ACL ligament

Compared to the first image this second one looks not that straightforward. The MRI shows an incomplete tear of the ACL ligament, that still represents a problem, however is difficult to grade the severity of the damage by the image itself.

Is in this situation where routine tests like the lachman and pivot shift test help the specialist providing information about the stability of the knee in motion. From what was shown in chapter 1, it can be established that the results of the lachman test can be related to the results of the test using the KT-1000 arthrometer[5]. Therefore can be stated that the KT-1000 helps to provide quantitative (anterior posterior

Figure 2.16: MRI, partial tear of ACL ligament

translation in millimeters) information to the lachman test.

Unlike the lachman test, at this point there is not a definitive instrument or tool used for the measurement of the pivot shift. The work shown in this thesis project tries to fill that gap by introducing a non-invasive prototype aimed to be used during the pivot shift maneuver to collect data about the test.

Recalling image 1.7, it is known that what makes particular this test is the application of valgus and rotational forces, which will be tracked using accelerometer and gyroscopes modules.

The concept is to implement two sensing modules, one placed in the patient's tibia and the other in the bottom of the femur. With this it is possible to take one point as reference and get differential acceleration readings representing the anterior posterior translation force applied during the test.

Both acceleration modules are connected to the Arduino board, which handles the data acquisition and performs the following calculation for each new sample:

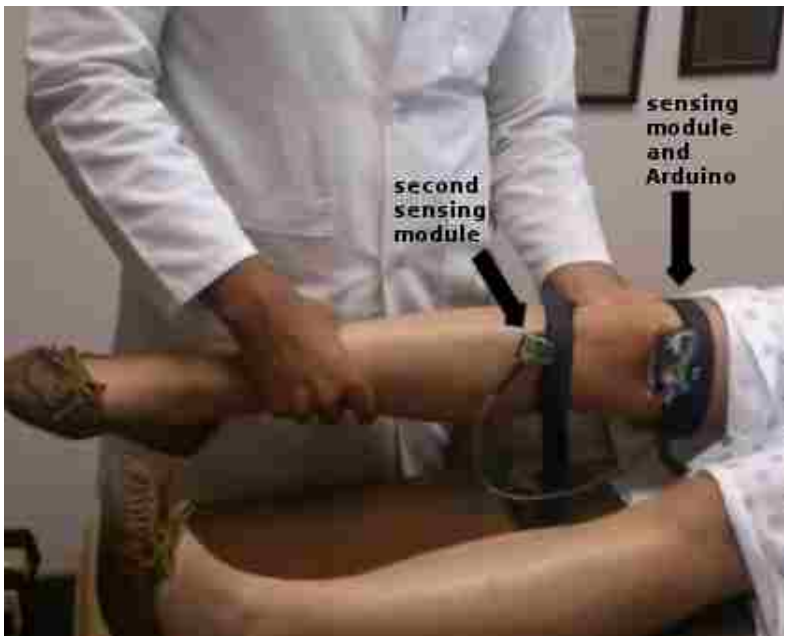

Figure 2.17: The pivot shift tester, one sensing module located in the tibia and the second one in the femur

$$\begin{aligned} Acc_x &= (Acc_{Xfemur} - Acc_{Xtibia}) \\ Acc_y &= (Acc_{Yfemur} - Acc_{Ytibia}) \\ Acc_z &= (Acc_{Zfemur} - Acc_{Ztibia}) \end{aligned} \tag{2.4}$$

where Acc_{Xfemur} is the acceleration output registered by the rightmost module on image 2.17 whereas Acc_{Xtibia} the one on the left side. Therefore Acc_x is the differential acceleration between femur and tibia during the test.

The prototype is powered up to a polymer lithium ion (LiPO) battery of 3.7V. While the test takes place the Arduino board sends the readings using the serial port interface, which makes the data accessible to other embedded system or computer.

The next chapter describes in detail how the data is presented to the user in real time (while the test happens) via an user interface created in the Processing programming language.

Chapter 3

The Pivot Shift Prototype: Software Design

In this chapter we explore the design and implementation of the software created to interact with the pivot shift prototype previously introduced. The application visually displays the readings from both the accelerometers and gyroscopes while the test takes place. The application was coded in the java based programming language Processing.

3.1 Processing

Processing is an open source, cross-platform programming language and integrated development environment initiated back in 2001 by Casey Reas and Benjamin Fry from the MIT Media Lab.

Initially intended as a introduction to programming for visual artists and designers, now has evolved to a development tool for professionals being used by students,

researchers and hobbyists alike.

Processing takes software concepts and transforms it to principles of visual form, motion and interaction. Within this visual context, Processing is set to work as a software sketchbook. The language is text based and implements a wide variety of functions and libraries aimed for computer graphics techniques like vector/raster drawing, color models, image processing, network communication, and object oriented programming. Custom made libraries can extend the functionality to generate sounds, send and receive data in different formats and enhance 2D and 3D file formats.

All programs created on Processing are a subclass of the PApplet Java class, additional classes are treated as inner classes when the code is translated to Java code before compilation.

Processing allows two main modes, the Java and Javascript mode, applications in Java are executed as a standalone window applet whereas the Javascript mode translates the code to work and run in a browser. Applications can be exported to Linux, Mac and Windows operating systems, with the option to embed Java runtime which is recommended to ensure the same performance between platforms.

Core libraries, and code used in the exported application and applets are licensed under GNU Lesser General Public License, allowing the programmer to release their code with license of choice[21].

There is extensive community support and resources to learn this programming language, recommended sites for this purpose are `https://processing.org` and `http://www.openprocessing.org`.

3.2 The Basics

Here we describe the particularities of the programs created in this programming language and a basic example, which will help to assimilate more easily the main application to be introduced later on [22].

In Processing, all sketches have two main functions:

- *setup*()
- *draw*()

The *setup*() function is called once during the execution of the sketch and it is used to initialize variables and run setup routines. The *draw*() function is the main loop of the application, and it runs automatically after *setup*() function, it should not be called explicitly. The function executes the lines of code contained inside its block until the application stops or *noLoop*() is called. The functions used to control the behavior of the main loop are:

- *noLoop*()
- *redraw*()
- *loop*()

If the main loop is stopped by *noLoop*() it can be reestablished using *loop*() or in the other hand if *redraw*() is called then the code inside *draw*() will be re-executed only one more time.

The following code snippet is an equivalent of a hello world for processing. This sketch will paint a point in the current position of the mouse cursor.

```
1  //Hello world
2  void setup() {
3          size(400, 400);
6          stroke(200,22,22);
7          strokeWeight(5);
8          background(200, 200, 200);
9          fill(240,20,20);
10         textSize(25);
11         text("Hello World",50,50);
12 }
13
14 void draw() {
15         point(mouseX, mouseY);
16 }
```

These is the result

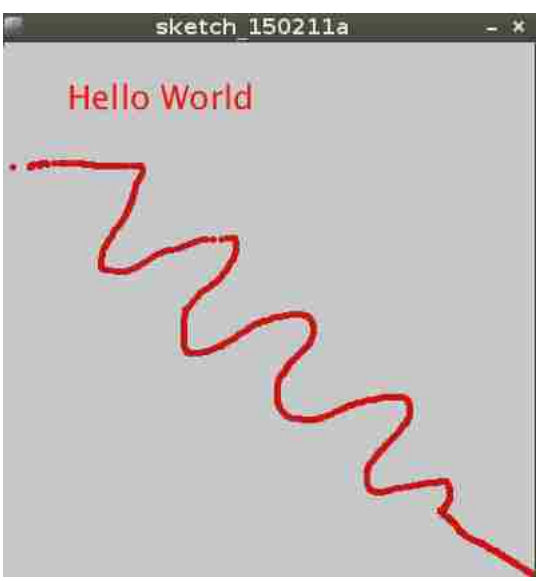

Figure 3.1: Simple application using Processing

Now that we showed the premise of programming in processing can go further and talk about the design of the pivot shift user interface software.

3.3 The Pivot Shift Software

The following diagram describes in high level the functionality of Processing's pivot shift application.

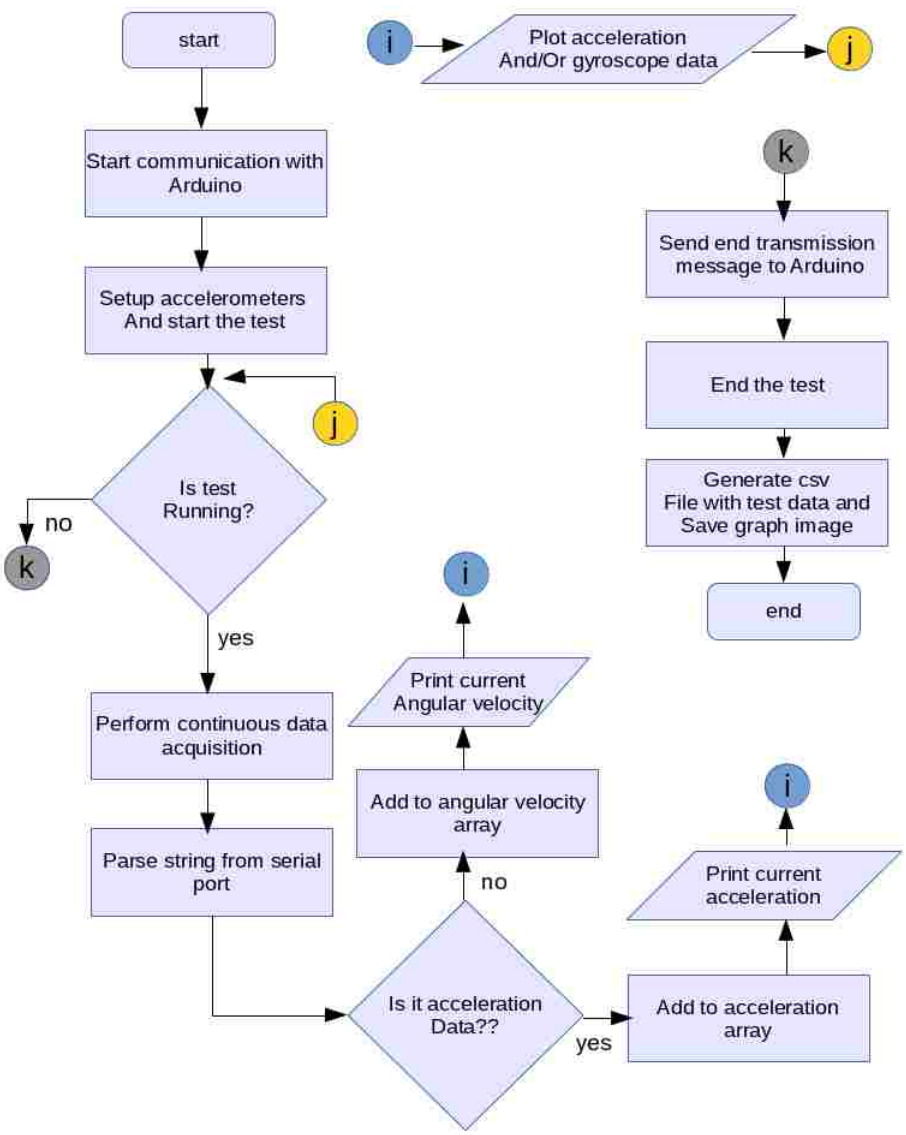

Figure 3.2: High level algorithm for pivot shift software

All starts establishing the communication with the embedded device, this is done via serial port. When using the Arduino board there are two options from which the serial port can be accessed, the first one via the digital pins 0 (RX) and 1 (TX), and the second one and the used in this project via USB. First there is a routine to check for the presence of a device connected in the serial port. After the device is found, then a pairing routine is executed. This routine establishes the the mode of operation for the test which consist of whether the user wants to use both sensing modules (to calculate differential metrics), or work with only one accelerometer. Once operation mode is defined a message is sent back to the embedded device to properly setup and initialize the sensors. Concluded the setup, the Arduino sends back a string specifying that is ready to start the test, at this point is in control of the Processing application to start the data acquisition.

The user begins the test via the user interface and starts to poll data from the sensors. While the test runs the acquired data is showed both in text format and by plotting a graph. Finally when the user stops the test an csv file containing all the readings from the test is saved along with a png image of the graph.

3.3.1 The Coding

Before starting coding the application few libraries are imported:

- processing.serial
- controlP5[23]
- java.io

processing.serial enables support for the serial port class, controlP5 is GUI and controller library that incorporates elements like sliders, buttons, toggles, knobs,

textfields among others to ease user interaction. This library is very convenient because Processing don't provide GUI elements out of the box although they can be manually implemented. The java.io library is used to manage filesystem capabilities and have access to local files and be able to save test results to disk.

Figure 3.3: A selection of controllers available with ControlP5 library

As was mentioned previously, the core structure of a Processing sketch is found in the functions *setup*() and *draw*(). Global variables are allowed as well, and they need to be declared outside the scope of *setup*() and *draw*() functions. Many global variables and classes are defined to setup the visual environment among other things including:

- initialize serial port class
- initialize ControlP5 class
- setup window size and color scheme
- define text labels and plotting area position and defaults

- setting default operation mode:
  - 1 accelerometer
  - 2 accelerometers
- plot mode:
  - acceleration only
  - accelerometer and gyroscope
- declare acceleration and rotation arrays

After global variables and classes are defined *setup*() is called and draws the initial user interface positioning text labels, plotting area and GUI elements like buttons and toggles, as well as looking for a connected device in the serial port. At the end of *setup*() execution we end up with this:

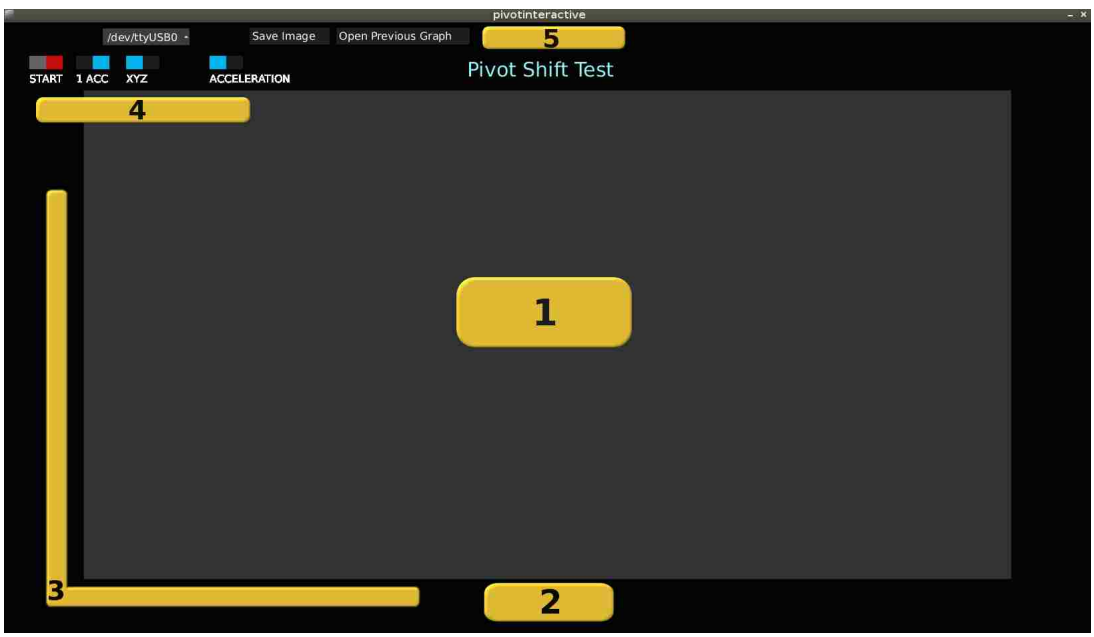

Figure 3.4: User interface for the pivot shift tester

Figure 3.4 shows the initial state of the UI (user interface) at launch. At that point the UI can be defined in 5 blocks showed as yellow rectangles, the first block indicates the area where the graph will be drawn, block number two is the area where text labels are placed to indicate the current metric e.g. for acceleration can be "x 1.25 , y 2.00, z .98" to specify current g values in each axis. Block three is the area where y axis (acceleration or rotation) and x axis (number of samples) labels are set for the graph. Fourth block contains four toggle buttons:

- Start-Stop. Used to begin and end the test
- Operation mode. Sets up the test to use one or two accelerometers.
- Enable Magnitude. Switches the graph to display each axis as its own curve or enables a single curve showing the magnitude of the three components.
- Graph Mode. Toggles view mode to display acceleration only or acceleration and rotation in a single view.

finally block five contains a dropdown menu to select serial port (in case more than one device is using the port), a Save image button that saves both an image of the test and an csv file containing all the data generated during the test. Open previous graph button allows the user to open an csv file from a previous test and display its graph.

3.3.2 Beginning the test

Once the application is launched and the visual environment is setup, then the serial communication between the embedded system and the PC begins.

```
1 Serial myPort;
2 try{
```

```
3           myPort = new Serial(this, portName, 19200);
4           myPort.bufferUntil('\n');
7           println("Starting test");}
8    catch(Exception e){
9             println("No serial port available");
10          }
```

This sample code initializes the serial port using a baud rate of 19200 bps. The variable portName holds the name of the serial port selected from the dropdown menu located in the upper left part of the UI. At this point the embedded system waits to receive some initialization strings from the serial port indicating how many accelerometers to use and when to start sending sensor data.

```
1    if(theEvent.controller().name()=="start")//Start the test
2    {
3      if(start==true)
4      {
5      timestart=millis();
6           if(first_time==true)
7           {
8           println("Selected serial port "+ dropDownItemName);
9           portName = dropDownItemName;
10          myPort = new Serial(this, portName, 19200);
11          }
12          Cleargraph();          //clear data arrays to start new
              test
13          first_time=false;
14          myPort.bufferUntil('\n');
15          if(opMode==true){        //opMode-Operation mode
16          myPort.write('b');       //2 accelerometers mode
17          myPort.write('1');
18          }
19          else{
20          myPort.write('a');       //1 accelerometer mode
21          myPort.write('1');
22          }
23     }
24   }
```

This code is executed when the event on the Start toggle is activated (when pressed), it checks the state of the other toggle called OpMode (right next to Start toggle) to see if the user chose one accelerometer or two. A boolean value true for OpMode means using two accelerometers, as false specifies to use only one. Now the embedded system expects two strings, the first one indicates the mode 'a' for 1 accelerometer and 'b' for two, and a start/stop flag used to begin or finalize the test, '1' starts as '0' terminates.

3.3.3 During the test

Once the embedded system starts sending data from the sensing modules the importance resides in properly display it and store it for future analysis.

The strings the Arduino sends including the sensor's readings have an specific format illustrated by the following examples, for acceleration these are valid strings:

- *x 1.26*
- *y 0.98*
- *z -1.08*

and for rotation:

- *gx 25.30*
- *gy 15.00*
- *gz 85.96*

where x, y, and z represent acceleration and gx, gy, and gz rotational metrics from the gyroscope. Therefore the string is formatted in a *'metric+space+value'* manner.

The strings are parsed during the serial port event in the application, dividing them in two sections, the first identifying the metric and axis that belongs to, and the last part is converted to a float specifying the magnitude.

```
1 if(sdata.indexOf("x")>=0)//x axis
2       {
3         sdata2=split(sdata,' ');
4         arrayx.add(float(sdata2[1]));
5       }
```

In this snippet *sdata* is the string containing the newest line of data from the serial port. The string then is separated into numerical and metric part.

Six global arrays are defined *arrayx, arrayy, arrayz, arraygx, arraygy, arraygz* each one storing the data for its corresponding metric and axis. This is how the application continuously stores the data coming from the embedded device, the next step once each of the metrics has at least one sample is to proceed with the display of the graph.

An additional array *arraytime* is used. This array keeps track of the minimum total of samples that all of the metrics have at a given point. The main reason for this is to know up to what number of sample the graph can be displayed. The following output displays the number of samples that each array haves at 4 seconds of elapsed time.

```
1 x:142 y:142 z:142 gx:142 gy:141 gz:142  ##elapsed test time
  :4.291s
```

For this example *arraytime* should have a value of 141.

As was showed, the plotting area is defined to use the majority of the UI space. In Processing the size of the application window is specified explicitly in most cases using pixels. In other approach it can be set to have a size based on the screen resolution, which makes the application not to depend on specific hardware. In this

application it is set to have a size of about 85% of the screen width and height. Then after size is defined two variables are automatically set *width* and *height* as we can see in the code:

```
1  size(round(displayWidth*.85), round(displayHeight*.85));
2  //Single graph layout
3  plotX1 = 120;
4  plotX2 = width - 120;
5  plotY1 = 100; //70
6  plotY2 = height - 85;
7  //Dual layout
8  plotY1_1=plotY1;
9  plotY2_1=plotY1+plotY2*.40; //end of first plot area
10 plotY1_2=plotY2_1+50; //start of second area for plot
11 plotY2_2=plotY1_2+plotY2*.40; //end of second plot area
```

the *size*() function takes two parameters being the width and height. What the code does is setting variables that represent corners of the rectangle enclosing the plotting area. As the application is set to show acceleration or acceleration and rotation, two layouts are predefined. This code is found inside the *setup* function called at the beginning of the sketch and having those dimensions already defined facilitates switching layout during runtime. The next screen-shot illustrates the position of the rectangle's vertices for the plotting areas. Function $rect(a, b, c, d)$ is used to draw the rectangles each parameter describing:

- a- x-coordinate of rectangle (upper left corner by default)
- b- y-coordinate of rectangle
- c- width of the rectangle
- d- height of the rectangle

Therefore, in order to draw rectangles for acceleration and rotation *rect*() needs to be called with parameters:

```
1   rect(plotX1, plotY1_1, plotX2, plotY2_1); //upper rectangle
     acceleration
4   rect(plotX1, plotY1_2, plotX2, plotY2_2); //bottom, rotation
```

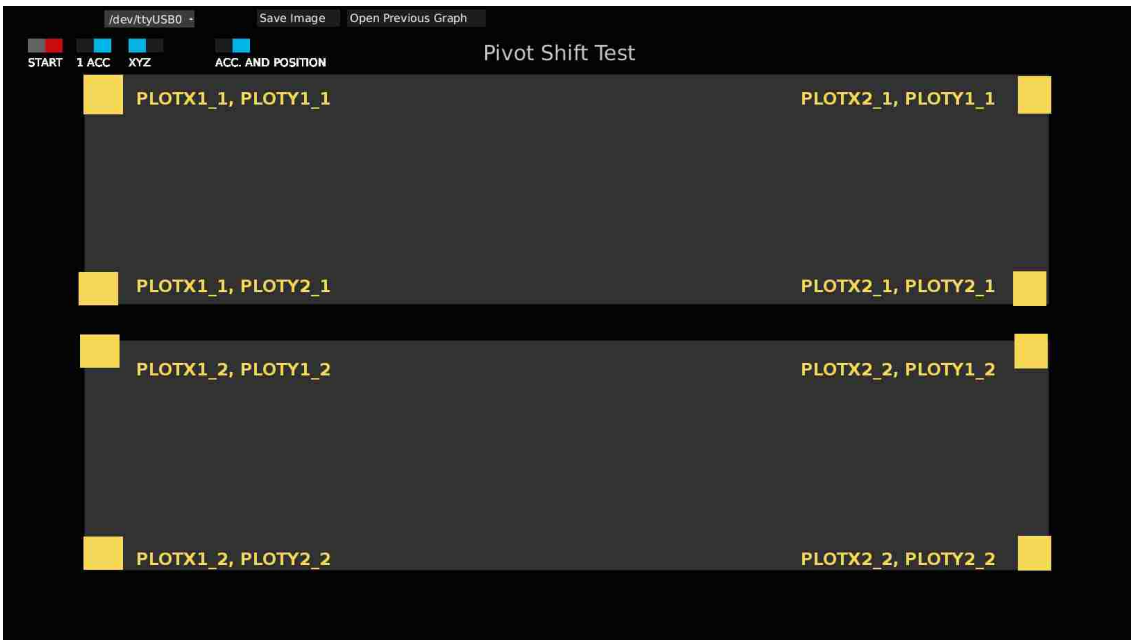

Figure 3.5: Pivot Shift UI, dual layout presentation

Now that the area to display the graphs is properly defined, it is time to map the values obtained from the sensors (acceleration and rotation) into the area enclosed by the rectangles.

The final graph for each of the metrics has as the Y axis the values for acceleration and rotation, as the X axis represents the number of samples for the test. To draw this line graph, sample i is connected with sample $i + 1$ by a line. To achieve this the first thing is to transform the value of the sample (acceleration or rotation value) to its corresponding pixel value inside the coordinate system created by the plotting rectangle.

This is done using the *map*() function:

```
3 float map ( float value ,float low1 , float high1 ,
4     float low2 , float high2 ) {
5 return high2 + ( high2 - low2 ) *(( value - low1 ) /( high1 -
   low1 ) )
6 }
```

where *value* stands for the number to map or transform, $low1$ and $high1$ are the minimum and maximum values in the original space, in this case, if the metric is acceleration then $low1$ should be the minimum value of all the acceleration samples stored so far, as $high1$ works in the same way taking the maximum. The arguments $low2$ and $high2$ represent the new range in which the value will be mapped into. In short, the function takes a numeric value and transforms it from the scale $low1-high1$ to a new value in the range from $low2 - high2$.

For example, if the current value for acceleration is 1.25 g's, then *map* function has to be called twice to get the corresponding X and Y position (in pixels) of the sample inside the plotting area.

```
1 xplot=map (1.25 ,1,arraytime.size(),plotx1,plotx2)  //X
   position in pixels
2 yplot=map (1.25 ,minval,maxval,ploty2,ploty1)   //Y position
   in pixels
```

For the X axis the original boundaries are between 1 (the minimum number of samples) and the total number of samples. The new range is defined by the width of the plotting area that is between $plotx1 - plotx2$. The Y axis goes from the range defined by the minimum and maximum acceleration values to the range between the points $ploty2 - ploty1$.

To finally reproduce the graph of the three axes in real time , a function called $Plotarray(arraytime, arraymetric, strokecolor)$ is defined. The first argument *arraytime* is the array holding the values for the horizontal axis, *arraymetric* can be one of six choices *arrayx, arrayy, arrayz, arraygx, arraygy*, or *arraygz* storing the

acceleration or rotation of one of the axes. The *strokecolor* parameter specifies the color of the line to be drawn. Therefore, in order to generate the continuous graph of the acceleration metric, the following piece of code needs to be called inside the *draw*() loop:

```
1 PlotArray(arraytime,arrayx,"R");
2 PlotArray(arraytime,arrayy,"G");
3 PlotArray(arraytime,arrayz,"B");
```

leading to a graph like this:

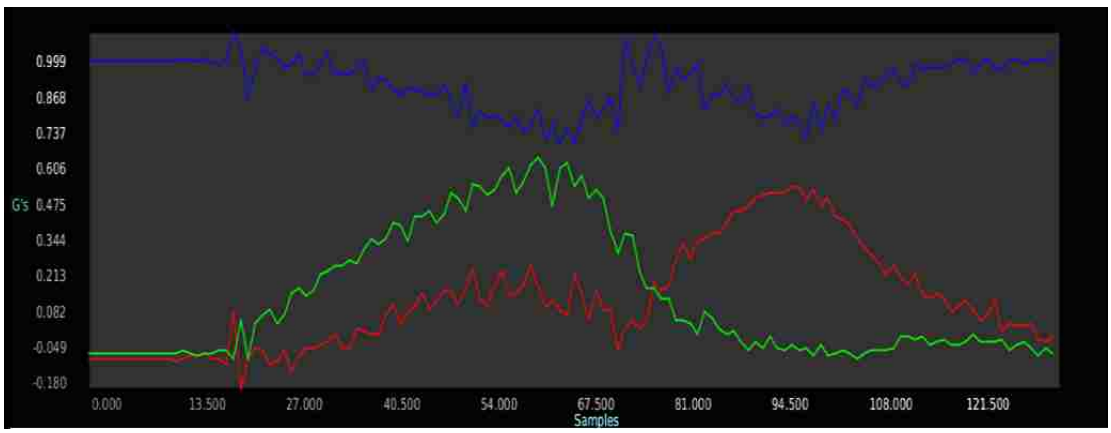

Figure 3.6: Sample acceleration graph: x axis in red, y axis green, and z axis in blue

since the *Plotarray*() function is called during the main loop, it automatically scales the graph to the values stored in the data arrays. The image shows the resulting acceleration (in g's) signals for each of the axes during the test.

3.3.4 From angular velocity to angular displacement

Recalling the features of the sensing module LSM9DS0 from the previous chapter, we know that incorporates both an accelerometer and a gyroscope. The acceleration is presented as g's while the angular velocity is presented in dps (degrees per second). Angular velocity is defined as the rate of change in angular displacement while

angular displacement is the angle through which a body is rotated in a specific sense (direction) and axis. This section shows the procedure taken to convert gyroscope output from angular velocity to angular displacement.

Directions for acceleration and angular rate are presented in the following image:

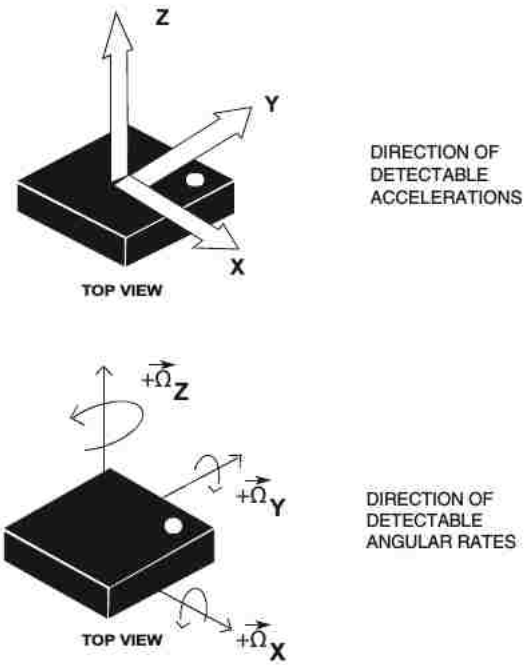

Figure 3.7: LSM9DS0 module: directions for acceleration and angular rates

the directions for rotation of each of the axes are presented, which are commonly known in flight dynamics like:

- roll: rotation in X axis
- pitch: rotation in Y axis
- yaw: rotation in Z axis

For this the Pivot Shift application it was considered to be more helpful to consider the angular displacement rather than the angular velocity. Using angular dis-

placement allows to clearly identify the directions which the prototype was rotated during test time, as it will be presented shortly.

Expressed in other terms, as we recall that the Pivot Shift maneuver takes both a valgus and rotational force, it is assumed that we can track the valgus force via acceleration while for rotation angular displacement is needed rather than velocity.

Now it will be compared the results of using angular velocity and angular displacement.

Figure 3.8: Sample test using angular velocity

Both of the tests showed by the graphs describe a similar motion as it can be seen from the acceleration plot (upper one). Initial state of the device is at rest in horizontal position, then it is rotated in an angle between 20° and 30° in the X axis (take figure 3.7 as reference).

Analyzing the first image showing angular velocity, can be seen how the angular speed picks up at the very moment that the object accelerates on the Y axis, after

Figure 3.9: Sample test using angular displacement

that point starts to lose velocity de-accelerating to return to its initial state. While this still is useful, it cannot provide information of the magnitude of the rotation, which is clearly seen in the subsequent image.

Looking at the graph using angular displacement, the movement done during the test can be reconstructed in some way, it can be said that while the device was positively rotated (rolled) about 23° it reached an acceleration on the Y axis about 0.374 g's.

The method used to transform the angular velocity to angular displacement involved adding the timestamp of each of the angular velocity samples got from the embedded device, in this way is known the difference in time between the current sample and the one received previously. To have that information the function *millis*() was used, which returns the number of milliseconds since the program started.

To provide the difference in time between samples two variables are used, one

representing sample i (current sample) and sample $i-1$ (previous sample). Once the difference between the samples is known, angular displacement can be described as:

$$Angle = \frac{(timestamp_i - timestamp_{i-1})}{1000} * AngularVel_i \tag{3.1}$$

where both timestamps are provided in milliseconds by the function $millis()$ and $AngularVel_i$ is the current angular rate (dps) provided by the gyroscope, and $Angle$ represents the angular displacement between sample i and sample $i-1$. Next table shows an example of how angular displacement is calculated in three consecutive samples. First column represents the timestamp difference between the two samples in seconds, the second column is the current angular rate coming from the gyroscope in dps, and the third column shows the resulting angular displacement (degrees) between consecutive samples.

$tgx_i - tgx_{i-1}(s)$	Angular Vel. (dps)	Angular displacement (°)
0.03	-1.71	-0.0513
0.03	-2.23	-0.0669
0.029	-1.78	-0.05162

Table 3.1: Conversion from angular velocity to angular displacement in X axis

3.3.5 Ending the test and storing data

Once the Pivot Shift maneuver has been performed the test can be terminated, to do so it's a matter of sending a string '0' to the Arduino executing the following line of code:

```
1 myPort.write('0');
```

when the Arduino receives the string stops sending sensing data and stays in an idle state waiting for the next test to start, sending a string '1' enables that.

At this point the user can save the test data on an csv file and a png image, in this way the graphs can be easily reproduced using an spreadsheet software and the data can be further analyzed.

Additionally to storing the acceleration and rotation metrics from each of the axes the software calculates the magnitude of both of the metrics to provide an additional graph in which the three axes are combined into a single signal, e.g. to calculate acceleration's magnitude:

$$acceleration_{mag} = \sqrt[2]{acceleration_X^2 + acceleration_Y^2 + acceleration_Z^2} \qquad (3.2)$$

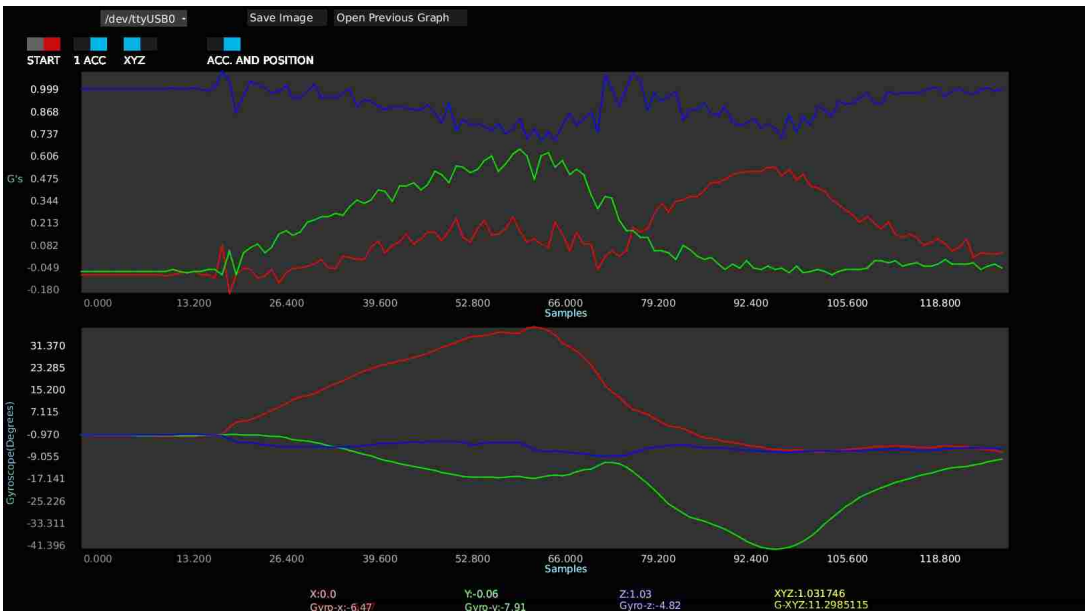

Figure 3.10: Sample test showing axes signals individually

where $acceleration_X, acceleration_Y$, and $acceleration_Z$ are acceleration samples for each of the axes. Figure 3.11 illustrates the magnitude for the acceleration and

rotation signals of the test coming from image 3.10.

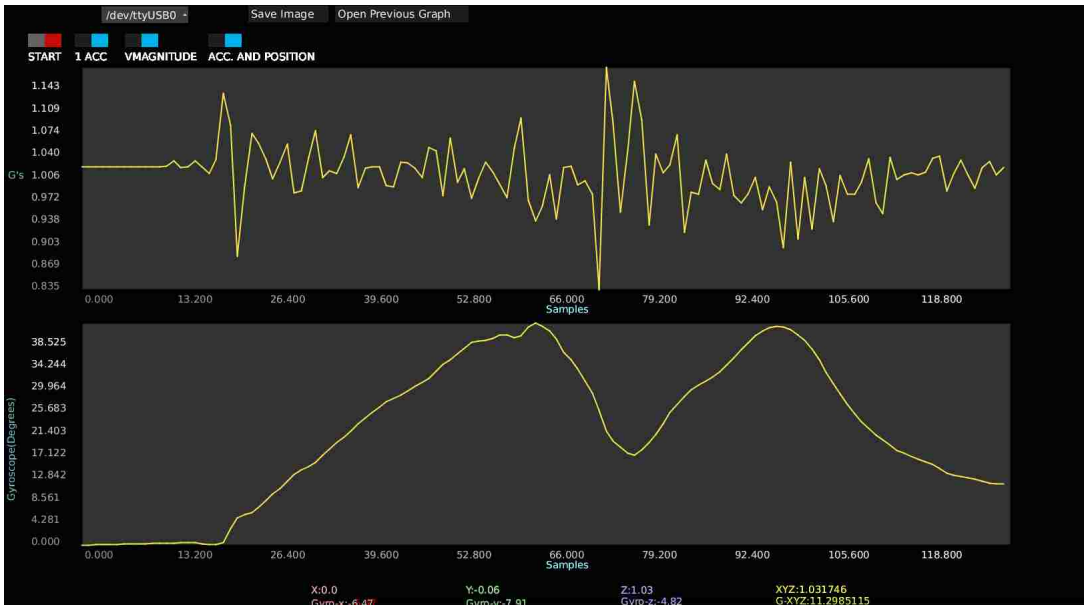

Figure 3.11: Sample test showing the magnitude for acceleration and angular displacement

Chapter 4

Clinical Trials

This section explains the origin of the previously collected data set used for the statistical analysis in this thesis.

Once the hardware and software were implemented, a completely functional prototype based in the first accelerometer MMA7361LC was handed off to a medical staff leaded by the orthopedist Edmundo Berumen Nafarrete M.D. and Carlos Vega Najera M.D. from the the Christus Murguerza hospital located in Chihuahua, Mexico with the goal of testing the prototype in clinical trials.

The inclusion criteria for this trials consisted on patients who attended orthopedic examination with the specialist and volunteer to be part of the study, no gender, age or specific medical conditions were restricted to the study.

The study group included a total of 156 patients, with mean age 24; range, 11-76 years; 37 women, 119 men. All patients participated voluntarily in the study by reading and signing a consent form approved by Christus Murguerza hospital ethics committee. Clinial trials took place from May 2013 to May 2014.

The study group can be further classified in three groups:

- healthy patients.
- patients with previous knee or leg condition unrelated to an ACL injury.
- patients with the ACL (anterior cruciate ligament) injury.

For this trails each patient was submitted to two clinical tests:

- pivot shift test
- KT-1000 test

The examiners group was small consisting of 2 physicians and the lead surgeon. Physician were instructed by lead surgeon on the execution of the pivot shift technique in order to perform the test as similarly as possible.

The pivot shift shift test was perform three times in each knee for every patient with the intention of assessing test repeatability. Patients with a previously confirmed ACL diagnosis where submitted to special treatment and had the test done under anesthesia.

For each of the patients, clinical evaluation of the pivot shift maneuver was determined manually by the physician and documented to keep track on patients with positive results (to later compare with prototype results). As for the prototype, patient's results consisted in two images and two csv files corresponding to each leg acceleration readings.

The KT-1000 test was perform in both of the patient's legs, documenting the individual result for each one as well as the absolute difference between legs, as described in chapter 1. This results were manually captured and stored on a spreadsheet file.

Figure 4.2 shows the resulting graph of the acceleration readings coming from the pivot shift test. The graph shows three noticeable maximum and minimum values

for each of the axis. These values are related to each of the three consecutive tests performed in the patient as described previously.

The specifications of the PC used with the prototype were the following:

```
##CPU DETAILS##############################
Architecture:          i686
CPU op-mode(s):        32-bit, 64-bit
Byte Order:            Little Endian
CPU(s):                2
On-line CPU(s) list:   0,1
Thread(s) per core:    1
Core(s) per socket:    2
Socket(s):             1
Vendor ID:             GenuineIntel
CPU family:            6
Model:                 15
Stepping:              6
CPU MHz:               2000.000
BogoMIPS:              3990.22
Virtualization:        VT-x
L1d cache:             32K
L1i cache:             32K
L2 cache:              4096K
##MEMORY#################################
             total       used       free
Mem:          2014       1610        403
-/+ buffers/cache:        933       1081
Swap:         2044          0       2044
```

Running Linux distribution:

```
 3.11.0-12-generic #19-Ubuntu SMP Wed Oct 9 16:12:00 UTC 2013
  i686 i686 i686 GNU/Linux

Distributor ID: LinuxMint
Description:  Linux Mint 16 Petra
Release:  16
Codename: petra
```

Next chapter introduces the results from testing the prototype on over a hundred

patients, performing a data analysis and final thoughts about the results.

Figure 4.1: Prototype used during pivot shift maneuver

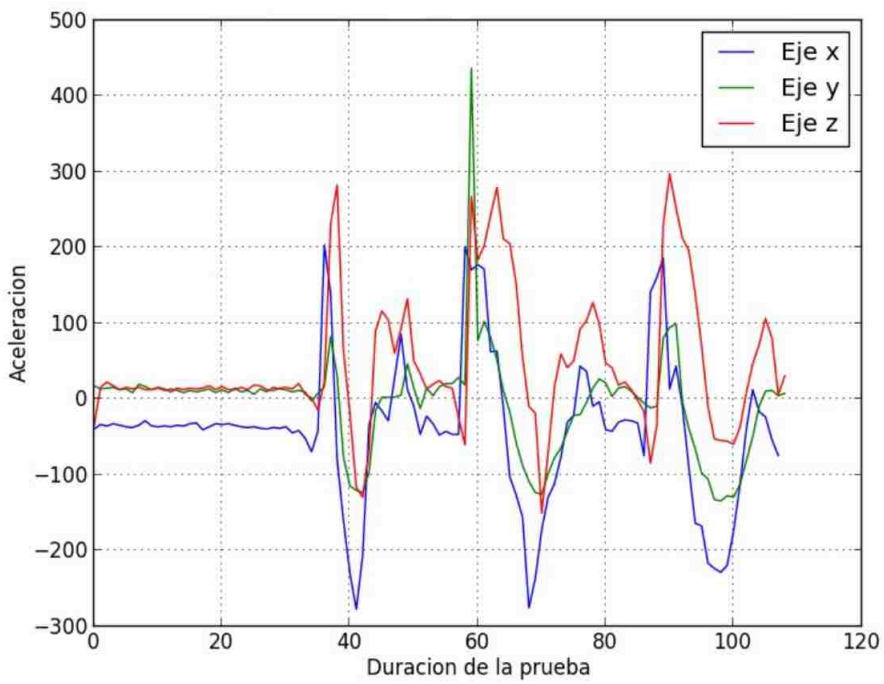

Figure 4.2: Graph showing acceleration output per axis from pivot shift test

Chapter 5

Data Acquisition and Analysis

This chapter takes the results of testing the pivot shift prototype with a study group of 156 patients, and analyzes the data files and graphs generated during these trials.

The data generated from the trails consisted in the following:

- 280 csv files
  - 140 for left leg
  - 140 for right leg
- 280 graphs
  - 140 for left leg
  - 140 for right leg
- a spreadsheet file containing patient data like: age, weight, KT-1000 test results, and patient observations

The total number of patients during the trials was 156, however inconsistencies where found in some of them like: missing tests results (csv file) for one of the legs,

user typos while naming the output file making the test impossible to relate to an specific patient. Due this complications some of the results had to be excluded in the following data analysis, leaving a total of 140 patients.

5.1 First glance at graphs and PyPlotter

At the time the data from patients became available, the first thing was to visually examine the group of graphs in order to get familiar with how real pivot shift tests acceleration graphs looked like. As well, a particularly interesting thing was to identify noticeable patterns or differences between the tests coming from left and right patient's legs. This is important because as was stated previously, given the direction of the movement, accelerometers can register both negative and positive acceleration for any of the given axis.

A Python/Qt[24] application was developed to ease this process of visual examination of the tests, featuring:

- Ability to reproduce graphs from csv files.
- Selectable axis, the user can display acceleration of three axis X, Y, and Z or choose which ones to use.
- Ability to overlap two graphs: useful to compare left and right legs in a same patient.
- Graphs can be zoomed and saved to png, svg, and pdf formats.
- Load all csv files from a given directory to easily plot different files.
- Works both for graphs produced by the MMA7361LC prototype (only acceleration) and LSM9DS0 prototype (acceleration + gyro).

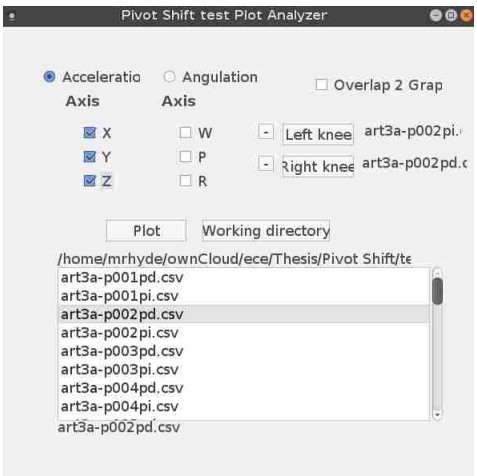

Figure 5.1: Pivot shift plot analyzer

with this, side to side comparison was done in patients to spot if obvious patterns were present. Next figure shows a patient left and right resulting acceleration graphs.

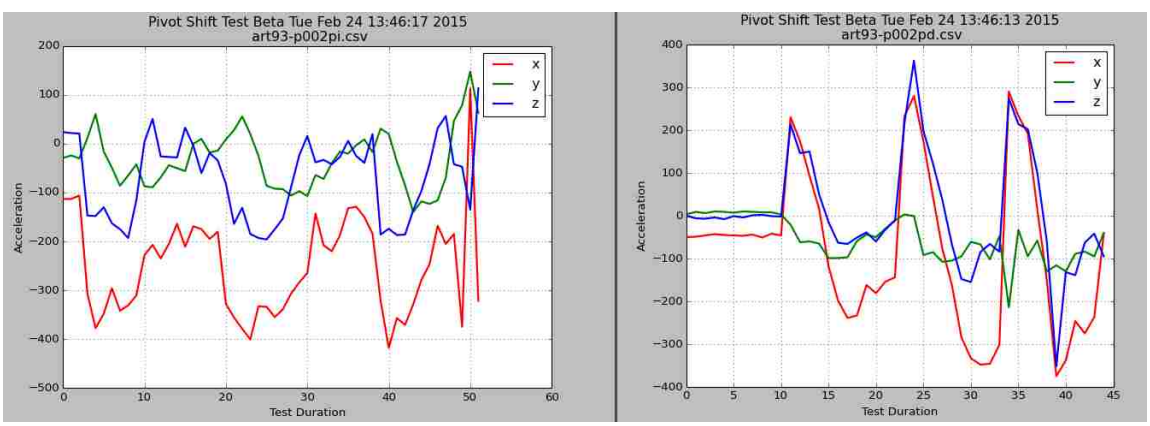

Figure 5.2: Patient graphs: left leg (left side), right leg (right side)

From this point on, for all upcoming XYZ acceleration graphs the color scheme used for each axis is:

- X axis: red
- Y axis: green

- Z axis: blue

Quickly looking at figure 5.2 is difficult to assess something at first glance. The recreation of the three consecutive pivot shift maneuvers is spotted without much effort as each of the axis presents 3 peaks or maximum points with similar values.

To compare left leg with right leg accelerations the following plots were done via the Python application:

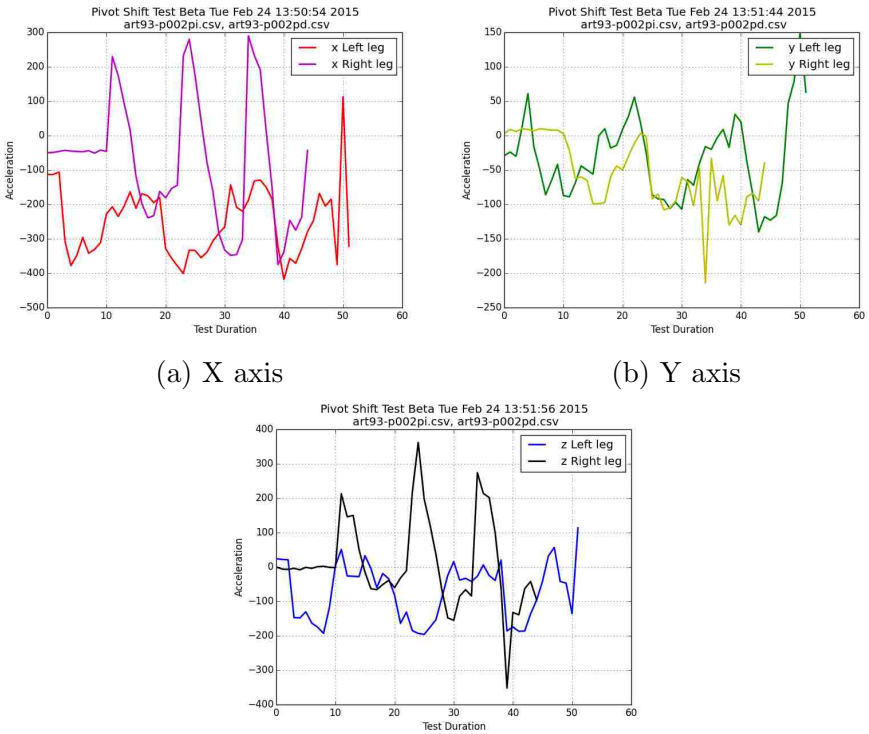

(a) X axis

(b) Y axis

(c) Z axis

Figure 5.3: Patient's side to side acceleration comparison for each axis

These group of plots show the acceleration differences on each of the axis (X, Y, Z) between left and right leg of the patient. Although one limitation of the data produced during the trails is noticed, left and right leg tests will not exactly match in the sense that do not equal in number of samples. This is caused due the fact

that is practically impossible for the the physician to execute both maneuvers (pivot shift for right and left leg) with the exact same timing, that is why an offset between the two tests can be seen as well. Despite this limitation, it will be shown how this overlapping plots still are useful for the analysis.

After reviewing this new graphs over several patients showing side to side comparison for each of the axis separately one thing became quite noticeable.

Recalling the pivot shift technique, we can consider its two main components as the rotation and valgus force applied to the knee. This rotation is called internal tibial rotation which makes reference to the direction in which the movement occurs and can be described as a rotation towards the direction of the other knee. That being said, e.g. the internal tibial rotation in the left leg is seen as rotating the leg towards the right leg.

Now that internal tibial rotation was defined we can go further and state the following: there should be a noticeable difference between patient's right and left leg pivot shift tests, the reason for this is that the rotation applied while performing the test on each side is opposite to its counter part.

Next graphs make clear this left to right side difference in rotation while the test takes place.

Figure 5.4 shows side to side acceleration graphs for the X axis on four different patients. Red curves correspond to left leg while magenta to right. Each of the graphs shows how right leg values tend to be considerably more positive than left ones. This effect on the X axis is produced mainly by two factors:

- difference in the direction of the rotation while performing the test on each leg
- the effect to the gravitational force going from the Z axis to the X axis while rotation happens

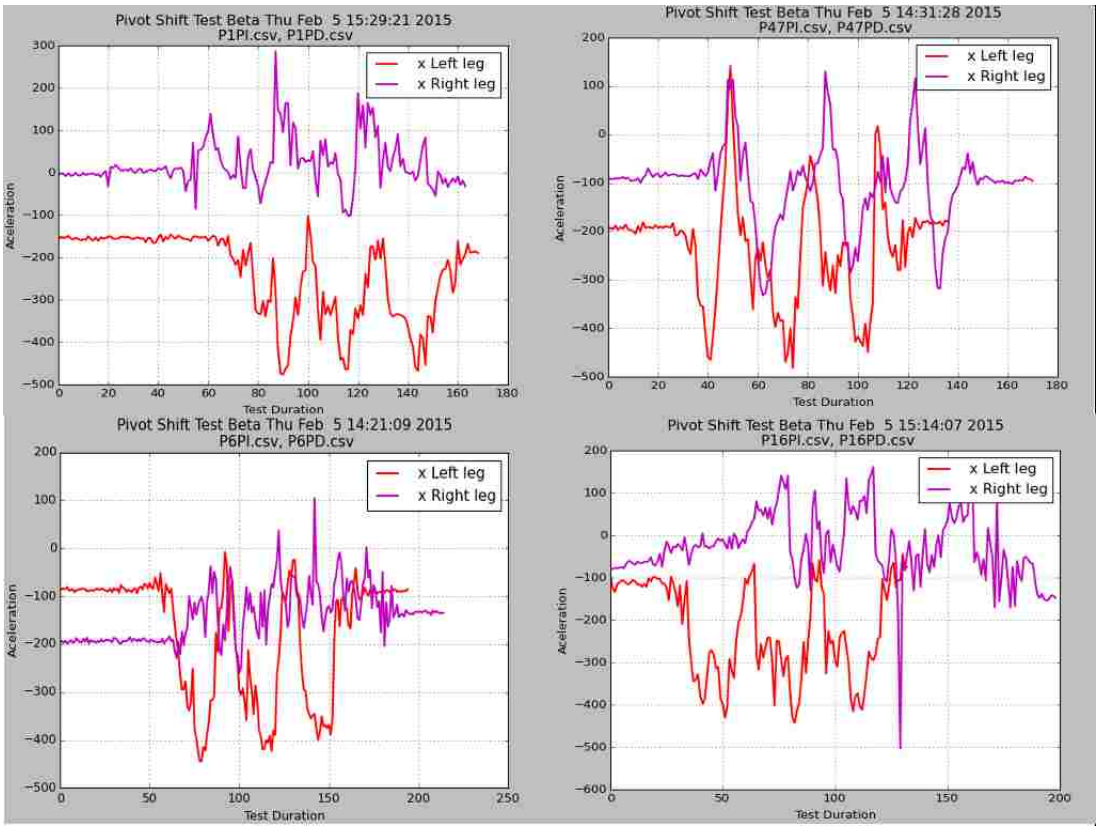

Figure 5.4: Side to side comparison for X axis in four different patients

Next section tries to describe the pivot shift movement and translate it to sections on the already presented acceleration graphs.

5.2 Interpretation of Graphical Data

This section breaks down portions of the graphs and relates them to parts of the pivot shift movement to help make sense of the shape found on the data.

The pivot shift maneuver can be divided en the following frames:

1. knee goes into extension

2. while extension application of tibial internal rotation

3. application of valgus force

4. flexion of the knee while applying both valgus and internal rotation

5. going back to knee joint extension

Figure 5.5 shows each of the movements produced during the pivot shift maneuver (just listed above). The bottom of the image works as reference to show the initial position and orientation that the accelerometer has when the test is about to start. This is critically important because keeps consistency on each axis among the tests. The way each of the axis is presented (bottom of the image) makes them relate to particular movements during the maneuver; in this case X axis handles the internal tibial rotation, Y axis the back and forth movement of the leg, and lastly the Z axis registers the knee flexion and extension. Due the importance of this, the prototype was marked to indicate to the physicians the correct way to align the accelerometers while conducting the tests.

Next to it the graph in figure 5.6 is the resulting left leg plot generated from the patient test shown in figure 5.5. Looking at it, can be seen how there is a similar pattern in the X and Y axis in portions of the graph, both axis have a negative bump followed by an increase in the acceleration on the Z axis. This pattern is clearly seen for each time the test was repeated in that graph (4 times). Relating this patterns with the movements during the pivot shift it can be established that the negative bumps coming from the X and Y axis are consequence of the knee rotation during the test. First there is the negative bump followed by a period of stabilization to similar values prior the rotation, and this has to do with the fact that close to the end of the test (frames 5 and 6) the knee reverts the rotation and extends to its natural position.

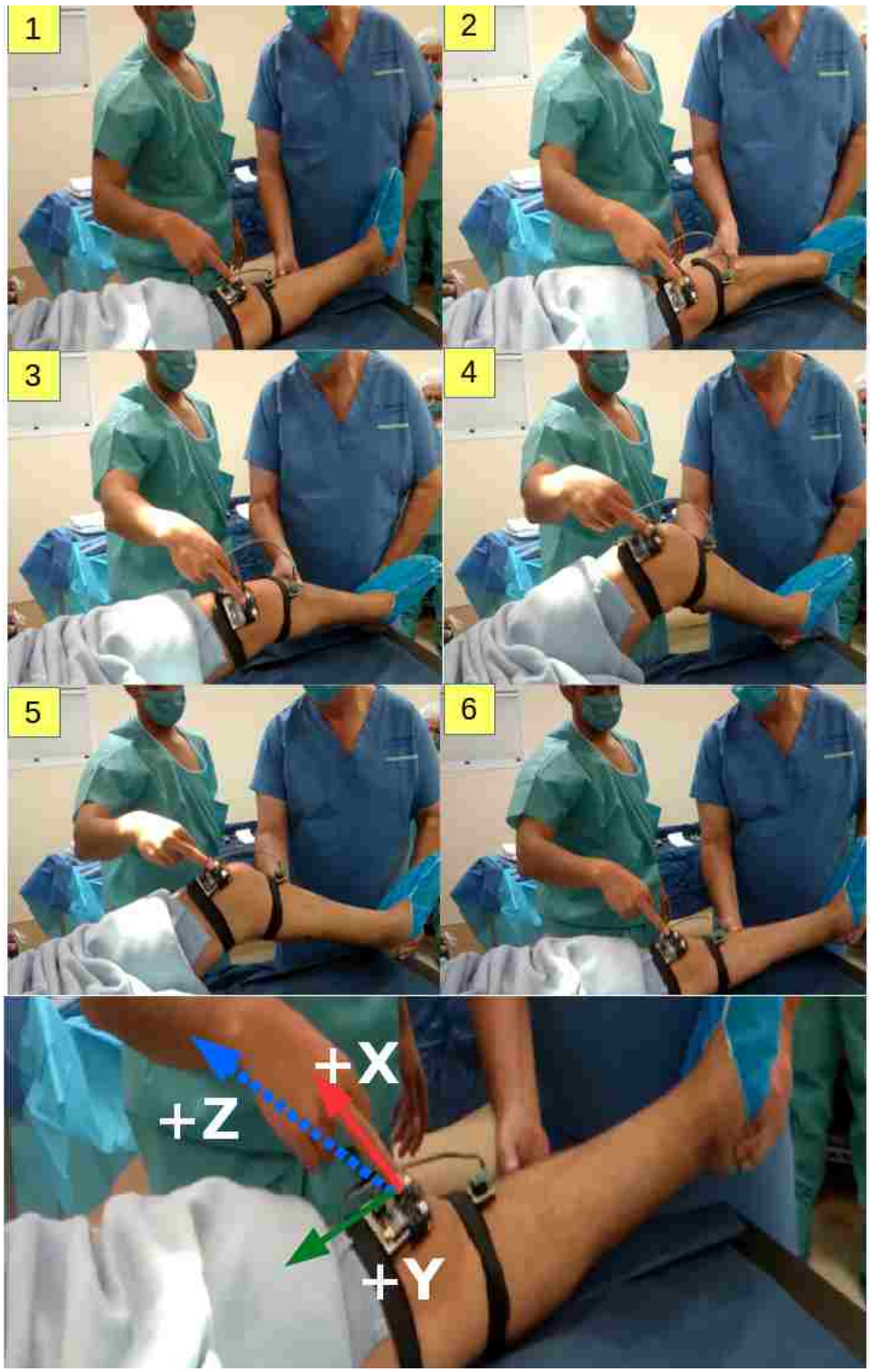

Figure 5.5: The pivot shift movement step by step, bottom describes positive directions for acceleration on each of the axis

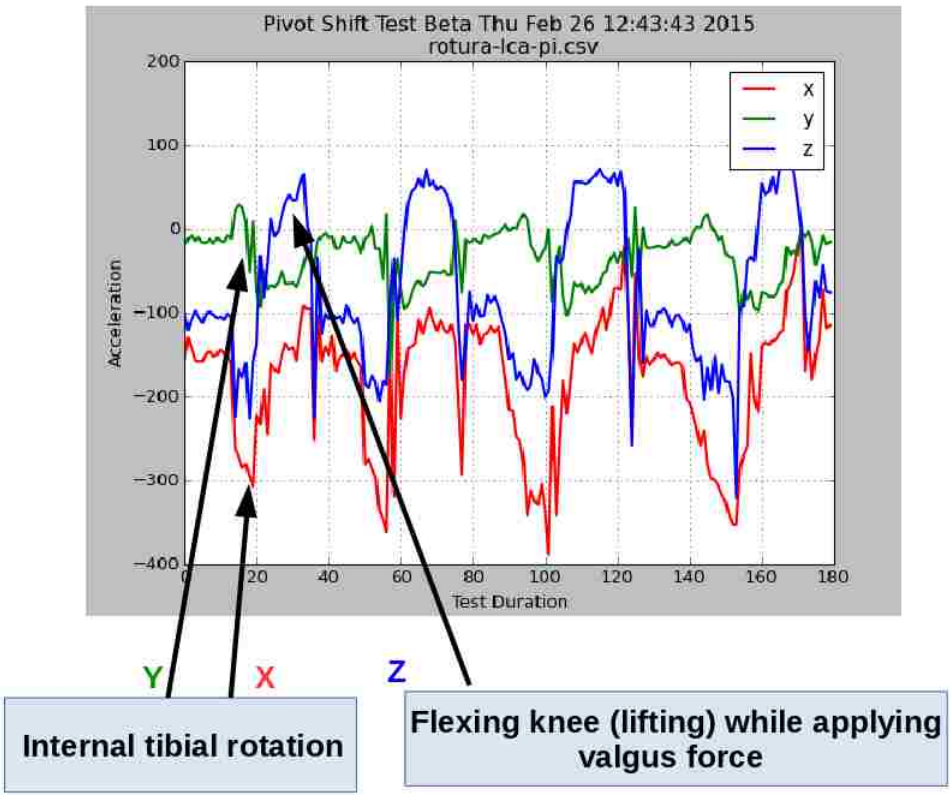

Figure 5.6: Interpretation of the maneuver

Regarding the Z axis, the initial values correspond to the leg in full extension (up to sample 12 approximately), after this internal rotation happens (frame 2) which slightly generates a negative acceleration on the Z axis (towards the floor) that can be seen in the graph by the minimum values seen between samples 13 to 20 approximately. Finally, once rotation is in place then the flexion happens (lifting the knee) generating the peaks around sample number 30. This Z axis dynamic repeats for this test four times as seen in the graph.

The image showed for this example was a left leg test. The same visual interpretation can be assumed for the right leg results taking in consideration the obvious difference between the internal tibial rotation reflected on the X axis from one leg to the other (they have opposite direction). As showed in previous side to side re-

sults in figure 5.4, left side rotation is measured as a -X acceleration, while its right counterpart as +X acceleration force.

5.3 Adjusting Left leg X axis readings

So far it has been stated that the most significant difference (visually) in the results of a pivot shift test between a left and right leg relates to difference found in the X axis results, which are produced by the direction of the internal tibial rotation that each knee has during the test.

Considering that many of the statistical calculations to be presented in following sections involve side to side comparisons of tests results, e.g. looking at the difference in maximum and minimum acceleration readings between legs or getting the mean value of the acceleration for all patients X axis (both legs). If those calculations were to be made taking the data as it is, it would be no problem in directly comparing side to side values taken from Y and Z axis since they tend to generate the same movement (from back and forth leg movement, and lifting leg towards flexion) whether the tests was from one leg or the other. Conversely, this represents a problem with the readings from the X axis since they will have the tendency to cancel each other due their opposite values. For this reason this section shows the method used to transform all the results taken from the X axis in left leg tests, in order to compensate the opposite rotation between legs. Once this done, it's possible to perform accurate side to side data comparisons involving X axis as well.

The function applied to perform this transformation is described as:

$$X(i) = -X(i) + 2(X_{initial}) \tag{5.1}$$

where X represents the array or vector containing al X axis samples and $X_{initial}$

stands for the first element or sample value in the array. This operation is done to all the samples in the X axis array with the exception of the first one, this due that the initial position for the device (accelerometer) in both legs (left and right) still is the same, this operation only tries to compensate the rotation, it does not mirrors the entire function horizontally which can be easily performed by doing $-X(i)$ as it will be showed.

The results of applying this operation have the form:

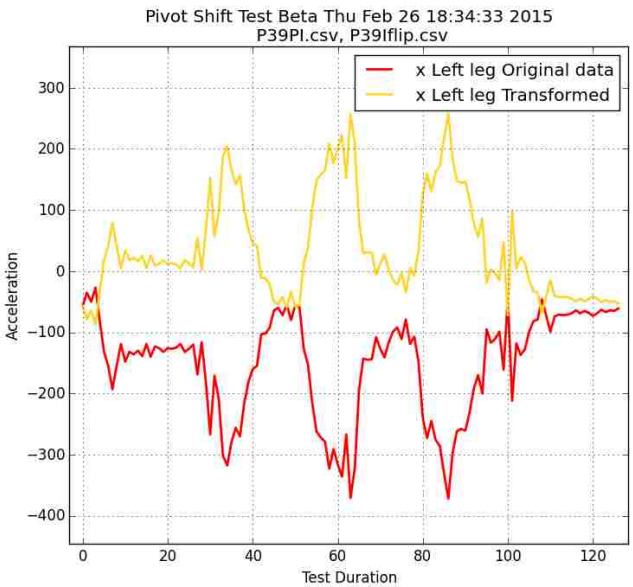

Figure 5.7: Compensation of internal tibial rotation for X axis readings

where the red signal is the original signal of a left leg test. As shown before, left leg internal rotation will be measured as a negative X axis acceleration, while a right one comes as positive.

Yellow signal corresponds to the result of applying the operation described by equation 5.1, which at the end creates the effect as if the rotation had the same direction for both left and right pivot shift tests.

Figure 5.8 shows the difference in comparing X axis results using the raw data and after compensating rotation.

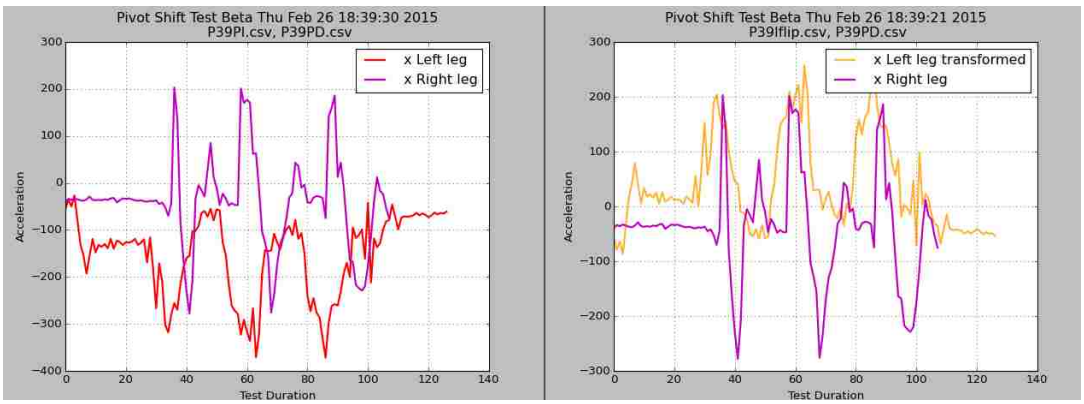

Figure 5.8: Side to side X axis comparison: left side with original data, right side compensating rotation

Analyzing the resulting graph (right side) it show how the magnitude of the acceleration for both maneuvers (left and right side) reaches similar maximum values. Now we can see how it makes more sense to perform this transformation prior to any side to side data comparison or metric calculation involving the entire dataset (three axis, both legs).

5.4 Transforming to G's

The resulting graphs presented up to this point share something in common that is, all of them have their acceleration values expressed in ADC (analog to digital converter) units, that is why the magnitudes can have a value of hundreds of units. Taking a step back down to chapter 2 of this work, it was defined that when using a 10 bit ADC (like the one used in this prototype based on the MMA7361LC accelerometer) the range of the output signal will have a value from 0 to 1023. Now, the reason why the results shown so far contain negative values and there is none

reaching this maximum 1023 is that since it is required to differentiate between positive and negative accelerations on each axis, a posterior calculation was made which will be explained shortly.

The way the output of the accelerometer (analog) operates is that if no input acceleration is applied, the output will reach a value equal to half the ADC range, in this case $1024/2 = 512$. In short, with no acceleration the expected output in ADC units should be 512 for each axis.

Other important fact is that from the ADC range half of all possible values are used to represent negative acceleration while the second handles positive acceleration. Therefore, by default values from 512 to 1023 reflect positive forces while ADC values from 0 to 511 negative accelerations. To make this negative and positive accelerations ADC units representation more straightforward the following calculation was performed for each sample:

$$ADC_{out} = ADC_{out} - 512 \tag{5.2}$$

this simple subtraction makes negative accelerations be in the 0 to -512 range and positive accelerations in the 0 to 512 range.

This explanation provides context to understand the reason behind the acceleration values shown so far, however in order to provide meaningful results to the calculations and metrics to be presented in the following sections it is required to step away from the ADC units and make use of an standard unit of acceleration. In this case the complete dataset was transformed to g's, remembering that $1g = 9.8m/s^2$.

Next snippet shows the function created to convert the complete dataset to g's using the R programming language.

```
3  ###CHANGE FROM ADC VALUES TO G'S FOR  MMA ACCELEROMETER#
4  ## call example: datahealthyG=togs(testdata_healthy) ###
5  togs<-function(dataset){
6    out=dataset
7    for(i in 1:length(dataset)){  #for each test file
8    ## (ADCVAL+512)*VREF/1023-ZEROV/SENSIBILITY
9      out[[i]][[1]]=sapply(dataset[[i]][,c(1)],function(i){ #Y
       values..
10       ((i+512)*(3.3/1023)-1.65)/.8})
11     out[[i]][[2]]=sapply(dataset[[i]][,c(2)],function(i){ #Y
       values..
12       ((i+512)*(3.3/1023)-1.65)/.8})
13     out[[i]][[3]]=sapply(dataset[[i]][,c(3)],function(i){ # Z
       values..
14       ((i+512)*(3.3/1023)-1.65)/.8})
15   }
16   out
17 }
```

This code applies the already covered procedure to get g's from chapter's 2 equation 2.3.

5.5 Tools and Packages used

The list of software packages and tools used to perform the majority of the calculations were the following:

- Python 2.7.9
  - python2-matplotlib 1.4.2-3 [25]
  - python2-numpy 1.9.1-1 [26]
- RStudio 0.98.1091
  - r 3.1.2-1

  - pysch 1.5.1 library [27]
  - Qt 4.8.6

- libreoffice 4.3.5.2

with hardware specifications:

```
[mrhyde@arch76 ~]$ lscpu
Architecture:          x86_64
CPU op-mode(s):        32-bit, 64-bit
Byte Order:            Little Endian
CPU(s):                8
On-line CPU(s) list:   0-7
Thread(s) per core:    2
Core(s) per socket:    4
Socket(s):             1
NUMA node(s):          1
Vendor ID:             GenuineIntel
CPU family:            6
Model:                 58
Model name:            Intel(R) Core(TM) i7-3740QM CPU @ 2.70
 GHz
Stepping:              9
CPU MHz:               3531.304
CPU max MHz:           3700.0000
CPU min MHz:           1200.0000
BogoMIPS:              5390.64
Virtualization:        VT-x
L1d cache:             32K
L1i cache:             32K
L2 cache:              256K
L3 cache:              6144K
NUMA node0 CPU(s):     0-7
Memory:                12G
```

running a Linux distribution:

```
Linux arch76 3.18.6-1-ARCH #1 SMP PREEMPT x86_64 GNU/Linux
LSB Version:  1.4
Distributor ID: Arch
Description:  Arch Linux
```

```
5 Release:  rolling
```

5.6 Data Statistics

This section starts to statistically described the data obtained from patients trials and considering that by this point two major operations have been perform to the orginal or raw dataset:

- X axis compensation (due internal tibial rotation)
- Conversion from ADC units to g's

The complete dataset consist of the right/left pair of csv files containing the tests results for 140 patients. As mentioned in chapter 4, each of the patients was clinically evaluated by the medical staff and classified the patients in three main groups: healthy, with observations and ACL patients. were patients with observations refer to those presenting some leg or knee previous condition unrelated to a torn ACL. Third group consisted on patients with ACL injury. The final distribution of the patients was the following:

ALL	Healthy	Observation	ACL
140	100	32	8

Table 5.1: Patients distribution

leaving a 71.4% of healthy patients, 22% patients with observations and 5.7% patients with ACL injury. The overall total of acceleration samples produced by the prototype during the 140 tests came to 27605 XYZ triplets; 18188 form healthy patients, 7128 patients with observations, and 2289 from ACL patients.

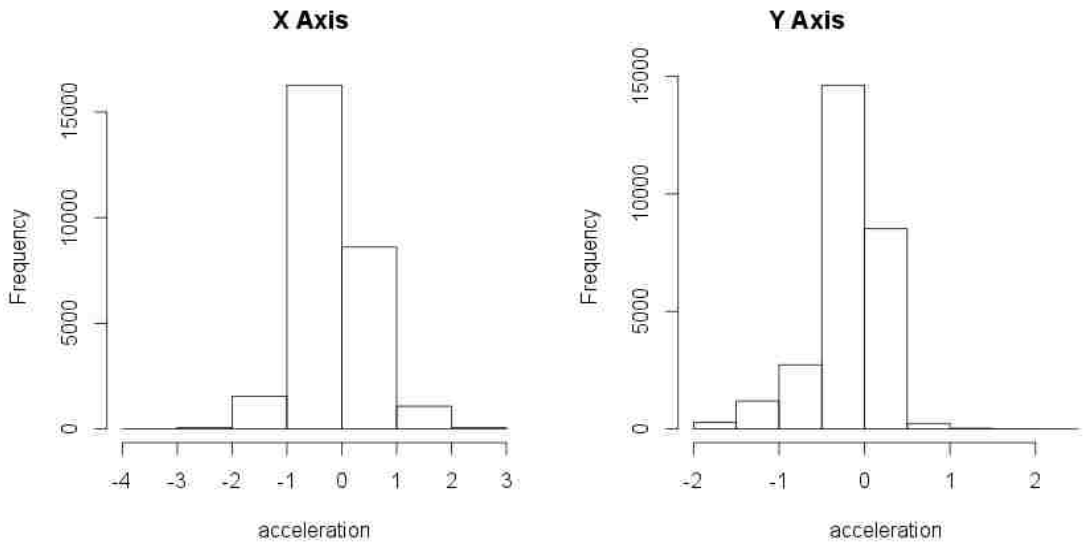

(a) X axis

(b) Y axis

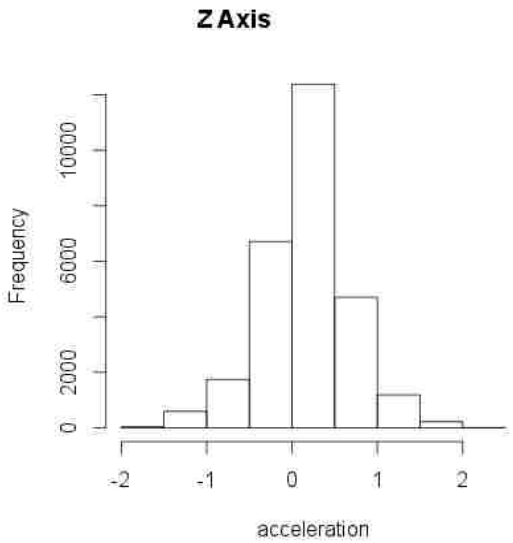

(c) Z axis

Figure 5.9: Histograms for complete dataset: a) X axis, b) Y axis, c) Z axis

From the histograms it can be show how for the X axis the majority of the data samples are between the 0g and -1g values, Y axis in the 0g to -0.5g range while the

Z axis does the same in the 0g-0.5g range.

axis	mean	sd	median	min	max	range	se
ALLX	-0.1448	0.5939	-0.1835	-3.2883	2.8085	6.0967	0.0035
ALLY	-0.1857	0.3759	-0.0746	-1.9294	2.0625	3.9919	0.0022
ALLZ	0.1708	0.5095	0.1835	-1.9738	2.0544	4.0282	0.0030

Table 5.2: Summary statistics for X, Y and Z data for all patients

variable	mean	sd	median	min	max	range	se
HX	-0.1561	0.5967	-0.2077	-2.5988	2.8085	5.4073	0.0044
HY	-0.1845	0.3721	-0.0827	-1.9254	2.0625	3.9879	0.0028
HZ	0.1311	0.5060	0.1391	-1.9657	2.0544	4.0202	0.0038
OX	-0.1392	0.6146	-0.1754	-3.2883	2.0262	5.3145	0.0073
OY	-0.2083	0.4002	-0.0665	-1.9294	1.5060	3.4355	0.0047
OZ	0.2468	0.5092	0.2923	-1.9738	2.0464	4.0202	0.0060
ACLX	-0.0728	0.4931	-0.0827	-2.3448	1.5020	3.8468	0.0103
ACLY	-0.1246	0.3153	-0.0262	-1.7399	1.8730	3.6129	0.0066
ACLZ	0.2499	0.5017	0.3246	-1.5665	1.9335	3.5000	0.0105

Table 5.3: Summary for X, Y and Z data for patients by groups

These previous tables describe the data of left leg and right leg results combined. Prefix H specifies healthy patients, O patients with observations and ACL patients with the ligament injury. From the data can be seen that both X and Y have negative mean values while Z stays positive. Out of the three axis Y is the one with the highest standard deviation. Graph 5.11 displays the same statistics but divided by healthy and ACL patients, from here it can be seen some differences in the mean value between axis.

These metrics like mean, maximum, and minimum values taken out of each group of patients (healthy and with the injury) will be used later on in this chapter with the goal of seeing if a patient can be recognized as a healthy or injured patient based on these reported values.

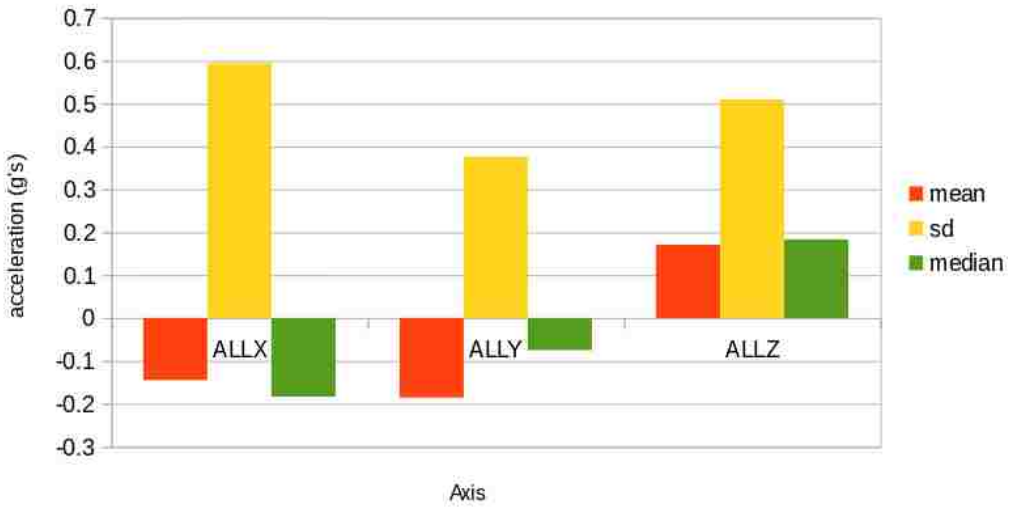

Figure 5.10: Mean, median and sd for complete data set by axis

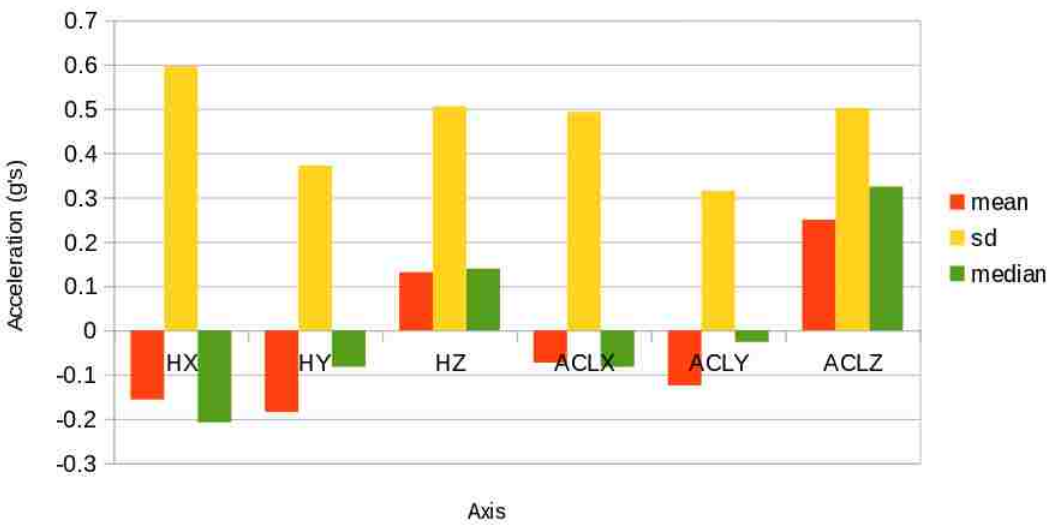

Figure 5.11: Mean, median and sd by healthy and ACL patients

Other metric calculated out of the tests was related to the maximum and minimum acceleration values registered during the pivot shift movement. As mentioned earlier, for each of the tests the pivot shift movement was reproduced three times in a row (reason why all the graphs present three similar spikes in the signal) in order to asses repeatability of the acceleration readings. Taken that into account there were some cases in which one of the three maximum or minimum values was significantly different in comparison of the other two.

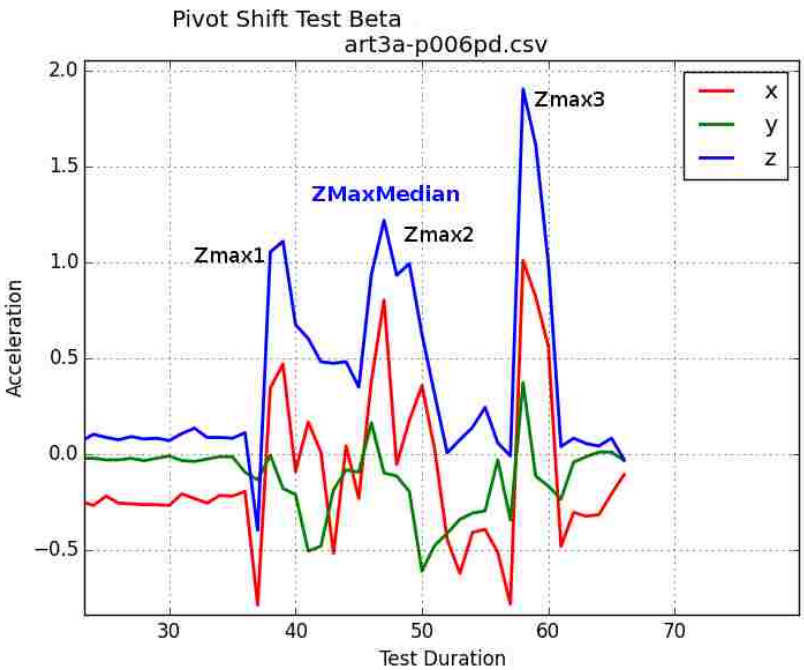

Figure 5.12: Taking the median of the maximum values

For this reason as shown in 5.12 it was decided to take the median of the maximum and minimum acceleration values while computing these metrics, e.g. while getting the maximum Z acceleration for the patient file used in this figure *art3a-p006pd.csv*, the reported value will be the median represented in this case by *Zmax2*. This prevents outline readings like Zmax3 to affect statistics in further calculations.

The metrics computed based in the maximum and minimum acceleration values per axis are displayed in table 5.4:

variable	mean	sd	median	min	max	range	se
ALLXmin	-0.9307	0.4683	-0.8952	-2.2722	0.6915	2.9637	0.0280
ALLXmax	0.8023	0.5497	0.8044	-1.4335	2.7802	4.2137	0.0329
ALLYmin	-0.8184	0.4252	-0.6976	-1.9214	0.0706	1.9919	0.0254
ALLYmax	0.2622	0.2283	0.2016	-0.1673	1.0948	1.2621	0.0136
ALLZmin	-0.6659	0.4306	-0.6391	-1.7278	0.3649	2.0927	0.0257
ALLZmax	0.9818	0.5261	0.9940	-0.3085	2.0181	2.3266	0.0314

Table 5.4: Maximum and minimum acceleration metrics

These calculations came from summarizing information like the one presented in the following table which shows the X, Y and Z maximum and minimum acceleration values per patient.

xmin	xmax	ymin	ymax	zmin	zmax	patient
-1.0222	0.3851	-0.8327	0.0020	-0.4859	2.0181	p001pd.csv
-0.9052	0.3891	-0.8488	0.2923	-0.8810	0.6794	p001pi.csv
-0.7923	0.9294	-0.4012	0.2964	-0.3367	1.6714	p002pd.csv
-0.7601	0.5383	-0.1794	0.2399	-0.7157	0.4657	p002pi.csv
-1.4778	0.8609	-1.3165	-0.0423	-0.3690	1.5665	p003pd.csv
-1.3488	0.4536	-0.5948	1.0544	-1.2117	0.4617	p003pi.csv
-0.8810	1.2762	-0.6956	0.0585	-0.3851	1.8367	p004pd.csv
-0.7762	0.4133	-0.3609	0.3972	-0.8448	0.8004	p004pi.csv
-1.0060	0.7117	-0.6754	0.5141	-0.4133	1.5060	p005pd.csv
-0.8407	0.1875	-0.1794	0.1956	-0.9133	0.1069	p005pi.csv

Table 5.5: Example table showing maximum and minimum values for 5 patients

5.6.1 Left and Right legs statistics

Unlike the test using the KT-1000 arthrometer that requires to be performed in both right en left legs to produce a diagnosis, the pivot shift test is able to asses the ACL

knee injury without testing both patient legs, for this reason further analysis shows the results from each legs separately.

Data is displayed for all patients as well as divided by healthy and injured groups:

variable	mean	sd	median	min	max	range	se
ALLX-L	-0.0582	0.6646	-0.1310	-3.2883	2.8085	6.0968	0.0057
ALLY-L	-0.1534	0.3501	-0.0625	-1.9294	2.0625	3.9919	0.0030
ALLZ-L	-0.0273	0.4797	0.0343	-1.9738	1.9214	3.8952	0.0041
ALLX-R	-0.2300	0.5007	-0.2198	-2.0544	2.0504	4.1048	0.0042
ALLY-R	-0.2174	0.3970	-0.0907	-1.8609	1.8770	3.7379	0.0034
ALLZ-R	0.3655	0.4606	0.3206	-1.9657	2.0544	4.0202	0.0039

Table 5.6: Summary statistics for X, Y and Z in left and right legs

One thing worth noticing is that even after performing the fix on left legs X axis data (compensating the rotation due contrary anterior posterior tibial rotation in section 5.3) still there is a significant difference in the mean values from left to right leg, which backs up the idea of performing the analysis in left and right legs separately.

variable	mean	sd	median	min	max	range	se
HX-L	-0.0682	0.6545	-0.1593	-2.5988	2.8085	5.4073	0.0068
HY-L	-0.1430	0.3494	-0.0665	-1.9254	2.0625	3.9879	0.0037
HZ-L	-0.0647	0.4623	-0.0101	-1.8810	1.9214	3.8024	0.0048
HX-R	-0.2447	0.5172	-0.2440	-2.0383	2.0504	4.0887	0.0054
HY-R	-0.2263	0.3893	-0.1069	-1.8609	1.8770	3.7379	0.0041
HZ-R	0.3285	0.4703	0.2762	-1.9657	2.0544	4.0202	0.0049
ACL_L-X	-0.5411	0.2660	-0.5988	-1.2319	0.7601	1.9919	0.0119
ACL_L-Y	-0.1291	0.3266	-0.0544	-1.0900	0.9300	2.0200	0.0146
ACL_L-Z	-0.2728	0.3223	-0.1900	-1.3327	0.4214	1.7540	0.0144
ACL_R-X	-0.1234	0.3550	-0.0948	-1.3044	1.2359	2.5403	0.0156
ACL_R-Y	-0.1690	0.4184	0.0060	-1.7077	1.8730	3.5806	0.0184
ACL_R-Z	0.3833	0.4401	0.3770	-1.5665	1.7440	3.3105	0.0194

Table 5.7: XYZ summary for patients by groups, left and right legs

And finally the data summarizing the average maximum and minimum acceleration values per leg by healthy and injured groups.

variable	mean	sd	median	min	max	range	se
HXmin-L	-0.7663	0.5299	-0.6935	-2.0948	0.6915	2.7863	0.0530
HXmax-L	0.7722	0.6167	0.7742	-0.5665	2.7802	3.3468	0.0617
HYmin-L	-0.6651	0.4028	-0.5464	-1.9214	0.0706	1.9919	0.0403
HYmax-L	0.2760	0.2030	0.2319	-0.0343	1.0544	1.0887	0.0203
HZmin-L	-0.9551	0.2837	-0.9597	-1.7278	-0.1714	1.5565	0.0284
HZmax-L	0.5715	0.3778	0.5101	-0.3085	1.5746	1.8831	0.0378
HXmin-R	-1.0793	0.3295	-1.0282	-1.8327	-0.3246	1.5081	0.0329
HXmax-R	0.8812	0.4036	0.8589	-0.3931	1.9778	2.3710	0.0404
HYmin-R	-0.8871	0.3879	-0.7843	-1.8165	-0.3327	1.4839	0.0388
HYmax-R	0.2474	0.2239	0.1875	-0.0706	0.9496	1.0202	0.0224
HZmin-R	-0.4163	0.3365	-0.3790	-1.6149	0.3649	1.9798	0.0336
HZmax-R	1.3745	0.2965	1.4234	0.7560	1.9536	1.1976	0.0296
ACLXmin-L	-0.9753	0.5346	-0.9172	-2.0867	-0.3528	1.7339	0.1890
ACLXmax-L	0.3891	0.7380	0.3448	-0.8206	1.4214	2.2419	0.2609
ACLYmin-L	-0.5599	0.3876	-0.4980	-1.1593	-0.1593	1.0000	0.1370
ACLYmax-L	0.2927	0.2866	0.1573	0.0948	0.8800	0.7852	0.1013
ACLZmin-L	-0.9959	0.3639	-1.0442	-1.5343	-0.4133	1.1210	0.1287
ACLZmax-L	0.3778	0.2829	0.2774	0.0867	0.7278	0.6411	0.1000
ACLXmin-R	-0.8458	0.2633	-0.8649	-1.2238	-0.4093	0.8145	0.0931
ACLXmax-R	0.8982	0.3452	0.9315	0.3891	1.4335	1.0444	0.1220
ACLYmin-R	-0.9526	0.4404	-0.9254	-1.6351	-0.3931	1.2419	0.1557
ACLYmax-R	0.3407	0.2695	0.2238	0.0907	0.8931	0.8024	0.0953
ACLZmin-R	-0.2273	0.2995	-0.2621	-0.6633	0.1673	0.8306	0.1059
ACLZmax-R	1.4068	0.2524	1.4315	1.0746	1.8770	0.8024	0.0892

Table 5.8: Maximum and minimum values for patients by groups, left and right legs

5.7 Classifying patients from data

After showing the statistic properties of the data from patient trails, this section focuses on seeing up to what degree is possible to tell from a healthy patient and

injured patient based on the metrics provided by the data presented in the previous section. Different approaches were taken in consideration from taking the mean, minimum, maximum or a combination of the three as main parameter to perform the classification.

The following experiments that we will call metric classifiers make use of the magnitude of the acceleration [28] can be define as follows:

$$Mag_{acc} = \sqrt{X^2 + Y^2 + Z^2} \tag{5.3}$$

which combines the three acceleration components into one.

5.7.1 Metric classifiers

The first attempt takes as main parameter the mean value of the acceleration presented on each of the patient groups.

variable	mean	sd	median	avg-min	avg-max	kurtosis	se
Mag_H_L	0.7603	0.4640	0.6664	0.2739	1.5847	2.0334	0.0049
Mag_H_R	0.8060	0.4577	0.7215	0.2666	1.7663	-0.1010	0.0048
Mag_ACL_L	0.7878	0.2098	0.7700	0.3478	1.1516	0.5318	0.0094
Mag_ACL_R	0.6655	0.4921	0.5348	0.1698	1.5837	-0.0985	0.0216

Table 5.9: Magnitude metrics summary for healthy and ACL patients

For example, *Mag_H_L* represents magnitude metrics for left leg healthy patients. The first metric (first column) in the table, is the result of taking the mean value of the acceleration in each of the patients, in this case the total hundred healthy patients and taking the average of that quantity.

The following snippet shows the coded function (Python) meanClassifier which was applied to all patient files which takes as an input the patient tests file (csv file generated from the software described in chapter 3) and the specification of if it is a right or left leg test file.

```
def meanClassifier(testfile, leg="left", mag="xyz"):
    print "filename: "+testfile
    data=getdataMag(testfile, mag)
    datamean=np.mean(data)
    meanaclL=0.7878379
    meanaclR=0.6654715
    meanHL=0.7603489
    meanHR=0.8060259
    #evaluate the test
    if leg=="left":
        delta_acl=abs(datamean-meanaclL)
        delta_h=abs(datamean-meanHL)
        if delta_acl<delta_h:
            print "DataMean:\t"+str(datamean)+"\t"+"MeanACL_L
             :\t"+str(meanaclL)+"\t"+"Delta_acl:\t"+str(
             delta_acl)+"\t"+"ACL"
        else:
            print "DataMean:\t"+str(datamean)+"\t"+"MeanH_L:\t
             "+str(meanHL)+"\t"+"Delta_h:\t"+str(delta_h)+"\t"
             +"Healthy"
    else:
        delta_acl=abs(datamean-meanaclR)
        delta_h=abs(datamean-meanHR)
        if delta_acl<delta_h:
            print  "DataMean:\t"+str(datamean)+"\t"+"MeanACL_R
             :\t"+str(meanaclR)+"\t"+"Delta_acl:\t"+str(
             delta_acl)+"\t"+"ACL"
        else:
            print "DataMean:\t"+str(datamean)+"\t"+"MeanH_R:\t
             "+str(meanHR)+"\t"+"Delta_h:\t"+str(delta_h)+"\t"
             +"Healthy"
```

The idea is simple, the function already contains the calculated mean values for healthy and ACL patients. The input files contain the X,Y, and Z acceleration readings for that particular pivot shift test, so the first thing is to calculate the

magnitude array (to get magnitude of the acceleration) that is handled by the *getdataMag()* function. The function contains as fixed parameters the calculated mean values for the ACL and healthy class (seen in the previous table). Then two variables are calculated *delta_ACL* and *delta_h* which are the absolute difference between the mean of the testing file (patient to classify) and the ACL and healthy means respectively. If *delta_h* is less than *delta_ACL* then the patient is classified as healthy, that is if the patient's mean is closer to a healthy patient mean.

Leg	Missclassified	Error %	Classifier
Left	55	40.41	MeanClassifier
Right	52	38.23	MeanClassifier
Left	94	69.11	MaxClassifier
Right	87	63.7	MaxClassifier
Left	91	66.91	MinMaxClassifier
Right	86	63.23	MinMaxClassifier
Left	90	66.17	MeanMaxClassifier
Right	90	66.17	MeanMaxClassifier

Table 5.10: Results of different metric based classification approaches

Previous table show the results of trying to classify patient data based on:

- mean value
- maximum value
- minimum and maximum values
- mean and maximum values

First column of the table specifies which leg the results are coming from, the second one (Missclassified) indicates the average number of patients that were incorrectly classified, and the third one shows the percentage that those missclassifications

represent out of the total number of patients. As can be seen clearly the error rate is too high, so a different approach was taken after trying this method.

Going back to what was shown in figure 5.5 while describing the pivot shift movement was mentioned the importance that X axis has while taking care of the acceleration during the internal tibial rotation as the Z axis registers the anterior posterior translation acceleration. Back and forth movement of the leg is assessed by the Y axis and could be considered as the least important feature of the three just mentioned during the pivot shift test[29].

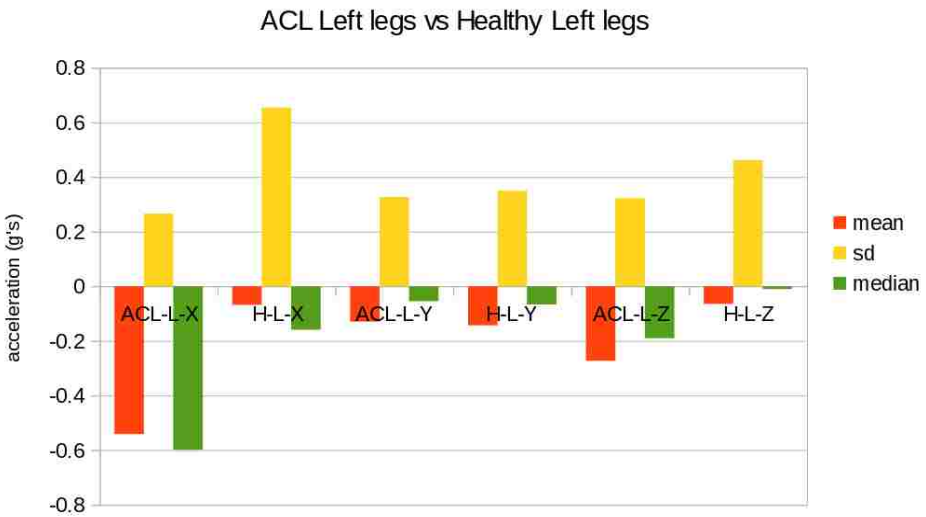

Figure 5.13: Left legs: mean, median and sd for ACL and healthy patients

Now, following this hypothesis and looking at graphs 5.13 and 5.14 we can see how it seems to be a noticeable difference in the ACL and healthy groups specifically in the X axis (most strong one) and Z axis. Seeing that and continuing with our emphazis of the importance of these two particular axis (XZ) the following try consisted in repeating the same metric classification methods but with the main difference of discarding Y axis. In this context the new magnitude was taken as follows:

$$MagXZ_{acc} = \sqrt{X^2 + Z^2} \tag{5.4}$$

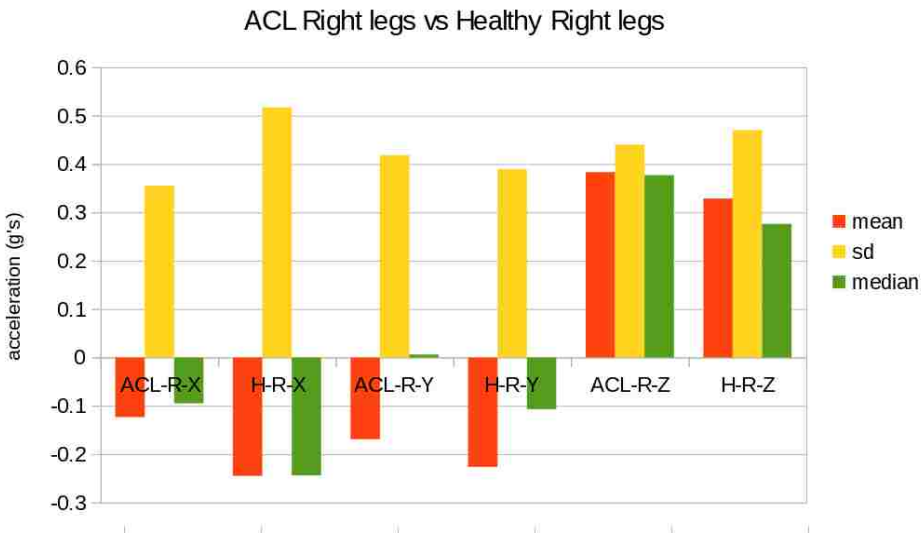

Figure 5.14: Right legs: mean, median and sd for ACL and healthy patients

Once done this, was needed to recalculate the same metrics (like in table 5.9)but this time based on XZ acceleration only, leading to:

variable	mean	sd	median	avg-min	avg-max	se
MagXZ-H-L	0.6916	0.4154	0.6176	0.2178	1.4774	0.0043
MagXZ-H-R	0.7038	0.4013	0.6283	0.2124	1.6750	0.0042
MagXZ-ACL-L	0.7051	0.2108	0.7043	0.2799	1.1495	0.0094
MagXZ-ACL-R	0.5721	0.3928	0.5199	0.1499	1.4425	0.0173

Table 5.11: MagnitudeXZ metrics summary for healthy and ACL patients

And the results of implementing the same classifiers was the following:

As simple as the change was from using the information from three axis to going to only XZ data, it's interesting to see how that effectively reduced the error rate almost in half for some of the proposed classifiers.

Leg	Misclassified	Error %	MagXZ Classifier
Left	57	41.91	MeanClassifier
Right	42	30.88	MeanClassifier
Left	45	33.08	MaxClassifier
Right	42	30.88	MaxClassifier
Left	46	33.82	MinMaxClassifier
Right	47	34.55	MinMaxClassifier
Left	46	33.82	MeanMaxClassifier
Right	43	31.61	MeanMaxClassifier

Table 5.12: XZ Magnitude metric classification results

5.7.2 Non parametric classification: K Nearest Neighbors

Previous section introduced some classification efforts purely based on statistical metrics pulled out of the testing data. As simplistic as they were they managed to be close to 70% accurate while classifying all the patients from the trails.

This section takes another approach towards trying to classify patients based on the data produced by the pivot shift prototype. The method implemented is a known algorithm commonly used in classification[30] and regression analysis.

The method used is the K nearest neighbors algorithm. To implement this algorithm and following the constrain of using the XZ acceleration data, we can say that the classification problem involves:

- 2 dimensions (X,Z)
- 2 classes (healthy, injured)

therefore the data coming from the patient trails is used in a different way this time, instead of looking at a patient file as a acceleration vs time graph, now it is seen as a collection of (X,Z) sample points where X takes the horizontal axis and Z the vertical one.

In this context, now we have two main XZ datasets one containing the samples for healthy patients and a second one for the injured class.

One major thing to consider is that the number of samples from healthy patients is clearly higher than the available on patients with the injury, and in order to accurately make use of the knn(k nearest neighbor) algorithm training data must be of equal size for all classes (this case healthy and ACL patients).

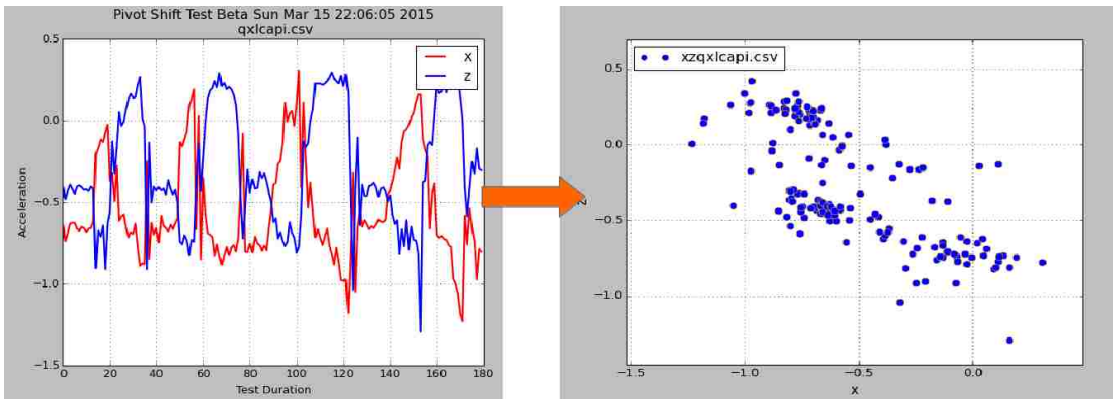

Figure 5.15: From (acceleration, time) to (X,Z) sample points

Figure 5.16 shows all the data available for the right leg. Red points are data for injured patient as black dots correspond to healthy ones. The total of points per class are:

- ACL 517
- healthy 9054

To overcome this difference in the total number of samples per class, the approach taken was to produce different subsets of the healthy dataset with equal number of samples to the ACL class, an example is shown in figure 5.17.

When classifying using the knn algorithm the output results in defining to what class each testing sample belongs to. This class is a result of a vote scheme in

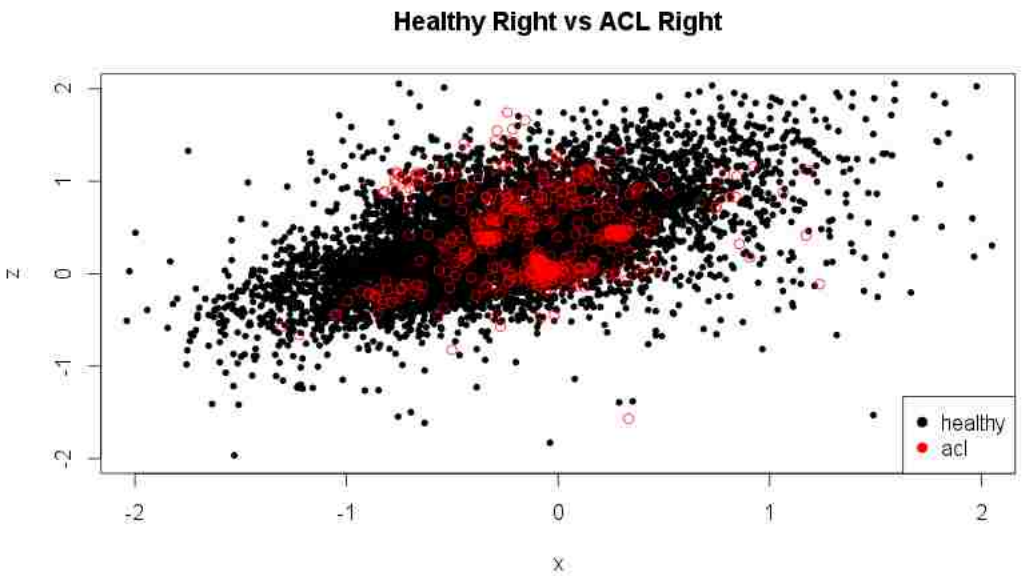

Figure 5.16: XZ datasets corresponding to right leg

which the object to classify calculates the k nearest samples to itself. The called or resulting class will be the one presenting the highest number of occurrences in those k neighbors.

Figure 5.18 illustrates an example in which one patient is being classified (right leg ACL patient). The upper left image shows the training sets for both classes (healthy and injured), upper right image adds to it the testing set corresponding to the patient to be classified (blue).

The image at the bottom contains a portion of the upper right figure (zoomed). Here we can see a testing point (in blue). If we were to apply knn with k parameter equal to 3 the resulting class would be the ACL or injured class, this because out of the 3 nearest neighbors to the sample point 2 belong to the injured class and only one to the healthy class, therefore ACL is the class with more occurrences in the neighbors. Due this voting nature of the algorithm is recommended to use only odd

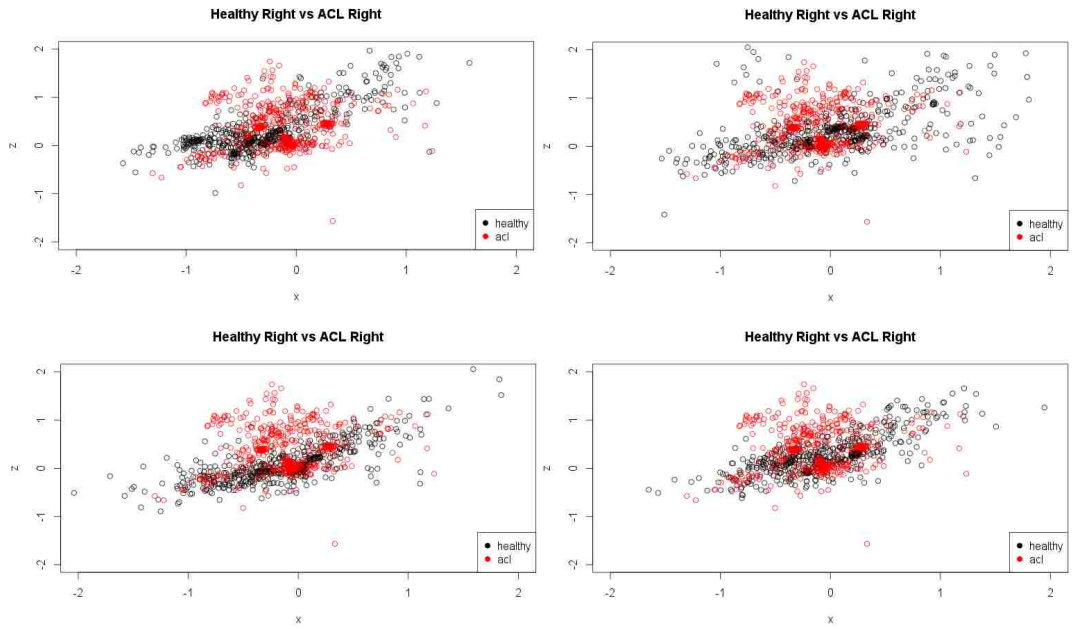

Figure 5.17: Creating subsets of the healthy class with equal size of ACL class

numbers as k parameter in order to avoid ties.

For this particular example, can be seen how even setting k to 5 produces the same result classifying that sample as part of the injured class. These are the classification results for that particular patient when k=3.

That specific test file contains a total of 170 XZ samples, out of which 17 were classified as healthy and 153 as ACL. The result accurately classified the patient as injured (patient P12 was indeed an injured patient) having an error rate of 10 percent. For this example k was set to 3 for illustrative purposes, in theory knn algorithm is said to be optimal as k goes to infinity[30] but to do so infinite data would need to be available, so in practice our selection on the k value is totally dependent on the amount of data available. In either case for the following results our k value is bounded to half of the training set. For each of the patients tested knn algorithm was run recursively starting from setting k equal to 1 up to half the

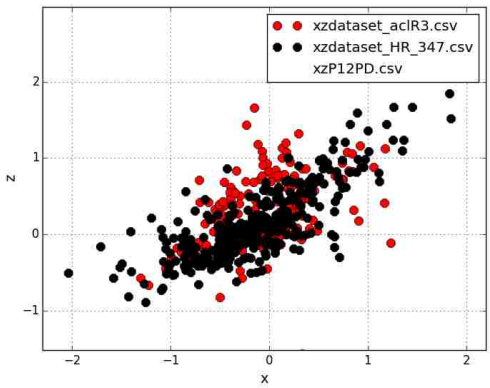

(a) Training sets

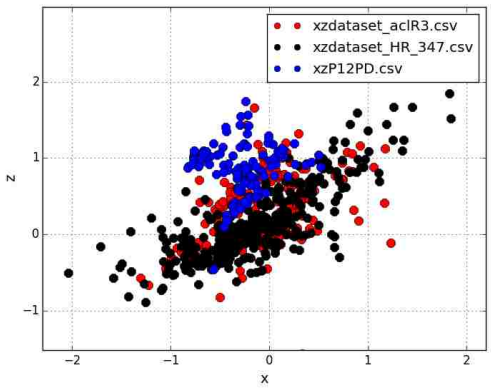

(b) Training sets and testing set (blue)

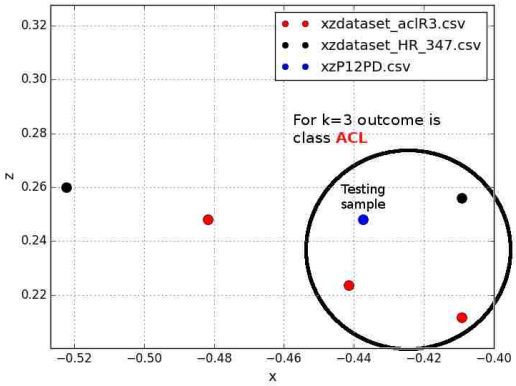

(c) Zoomed plot: example knn with k=3

Figure 5.18: Testing and training set examples

training set, the final classification results were the one reporting the minimum error rate. For example the results just seen from P12 were k=3 with an error rate equal to 10%. Optimal result obtained for this patient was using k=155 with an error rate of 1.76% (this patient did pretty good).

Tables 5.13 and 5.14 are the results obtained while classifying all the patients both right and left legs using knn rule.

From the results we have that for the right leg the average number of patients

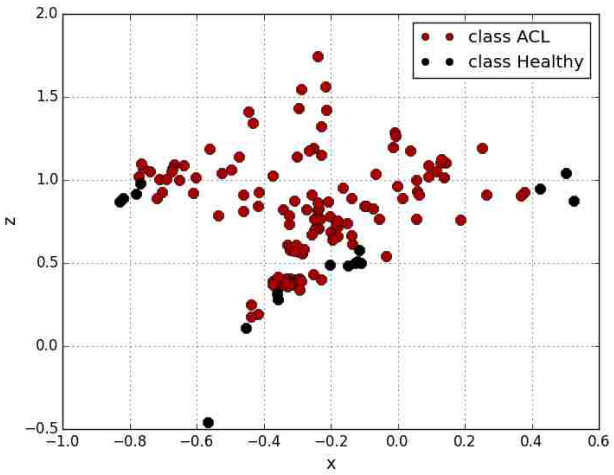

Figure 5.19: Classification results for patient file P12PD

	avg # patients	%
Missclassified	34.7500	25.5515
Classified	101.0000	74.2647
Avg Error		26.5699
Avg Error Class		10.8085
Avg Error Miss		68.5398
+ 70% accurate	86.7500	63.7868

Table 5.13: KNN results for Left leg

missclassified was of 15.07% and 25.55% for left legs. The mean average error rate for all patients was around 26%, this is considering all outputs both classified and missclassified results. The metric *Avg. Error Class* represents the mean error rate present in the patients correctly classified as *Avg. Error Miss* does the same for the missclassified part. The last metric from the tables specifies the percentage of patients that were correctly classified with more than 70% confidence or in other words less than 30% error rate.

Next are the average error rates per class. The first column specifies the average number of patients missclassified taking in consideration that there were a total of

	avg # patients	%
Missclassified	20.5000	15.0735
Classified	115.5000	84.9265
Avg Error		26.3211
Avg Error Class		20.5500
Avg Error Miss		54.3915
+ 70% accurate	62.8333	46.2010

Table 5.14: KNN results for Right leg

132 healthy patients and 8 with the injury, however out of those 8 patients 4 had the injury on the left leg as the other 4 on the right. For this reason previous tables had a total of patients of 136. The metric *avg class error* is the avg error rate that was present in the correctly classified tests and *avg miss error* is the same for the ones that were missclassified patients.

	avg # miss patients	miss %	avg class error	avg miss error	leg
H	34.75	26.3257	0.1096	0.6854	left
ACL	0	0.0000	0.0720	0.0000	left
H	23.6	17.8787	0.2473	0.6616	right
ACL	1	25.0000	0.2256	0.5109	right

Table 5.15: KNN: missclassifications rates by groups

The average error found in the correct classified patients was of 16.36% including both legs and classes. Average error in the incorrectly classified patients was of 46.44% for both classes and legs. Regarding the ACL patients, all of the left legs were correctly classified (reason why *avg miss error* is zero) as the right counterpart missclassified 1 out of the 4 patients.

Chapter 6

Conclusion and Future Work

6.1 Limitations and Future Work

In the course of developing this project and specially at the moment of starting the patient trials and data analysis some limitations were found. The fact that this project involves both medical and engineering staff and that the prototype was finally implemented by the end user (medical team) really helped up the project towards future development, since the staff came up with several improvement ideas that would not have been identified if the prototype had not been implemented.

Some of them involved minor hardware changes in the prototype, like a reset button or the use of an LED to display battery status to little more complicated like going wireless since the prototype needed to be directly connected to the pc via an USB cable. This was resolved by adding a pair of XBEE modules[31] based on the IEEE 802.15.4 which are fairly ease to use.

As well there were software related observations like making the application able to generate the graph in real time to small UI details to make it more intuitive and

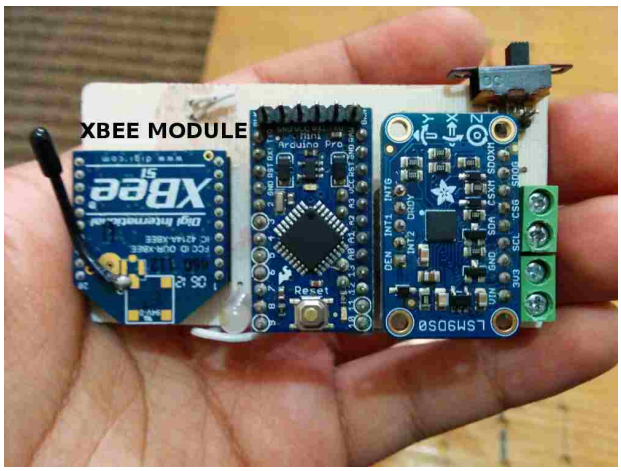

Figure 6.1: XBee module implementation

easy to use.

While starting looking at the resulting data from patient trials some design flaws were found. Two of the main ones were:

- The number of samples per tests was not the same
- Start of the actual test varied form patient to patient

These two observations became pretty evident at the begging of the data analysis, figure 6.2 shows tests results from left and right leg for the same patient. To begin with, it can be seen how one test has a total of samples for each axis of about 85 while the other leg has about 35. There were two factors that caused this, the first one was related to a software constrain in the application designed to capture the readings. The initial configuration of the application required the examiner to manually start and end the test using a button from the user interface (or a key shorcut), which automatically makes this disparity in sample size logical, it is highly improbable for the examiner to stop the test meticulously after an specific number of seconds every time. The second factor has to do with the actual execution of the

pivot shift maneuver. From examiner to examiner the technique may be the same but the timings or speed at which they perform it varies.

# of samples	left leg	right leg
mean	96.18	97.43
std	54.79	55.26
median	75	83

Table 6.1: Variability in sample size from test to test

The second observation it's clearly shown in 6.2a, the initial 35 samples (approximately) are acceleration readings prior of making the pivot shift test and are expected to exist in the results but for some files were considerably high. Since this initial samples do not represent acceleration readings caused by the actual medical test, they had to be manually removed from each file which added considerable time to the analysis.

To reduce the impact of these two findings in future, additions to the software were made:

- added a countdown prior of starting capturing data
- limited the test duration with a 10 second timer

The implementation of the countdown helped to reduce the number of initialization samples (before the actual movement) as automatically ending the test after 10 seconds helped to impose the examiner to a particular rhythm of execution and helped as well to ensure that all the tests have similar sample size. After the addition of the timer the average of samples per test is 215 samples $\pm$ 4 samples, fact that will help to facilitate further data analysis.

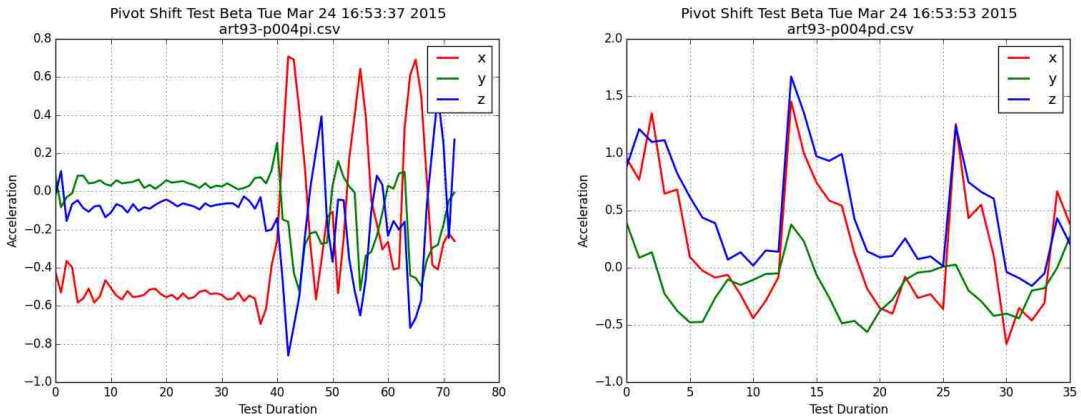

(a) patient left leg (b) patient right leg

Figure 6.2: Disparity in sample size and beginning of test

Figure 6.3: Recent test after software changes, 3/14/15

6.2 Conclusion

The project in this thesis introduces the design and implementation of an electronic device able to store quantifiable data out of the clinical pivot shift test. This test is considered a very valuable asset in the diagnose of the ACL (anterior cruciate ligament) injury and in the evaluation of its reconstruction surgery, however is often questioned over its subjective interpretation[32].

This debate over the subjectiveness of the test highlights the importance of having a device that produces quantifiable data out of this screening test. The successful implementation of the proposed prototype tries to fill that gap, providing numerical data in the form of acceleration and angular displacement that can be further analyzed.

Clinical trials were conducted in collaboration with the Christus Muguerza del Parque Hospital located in Chihuahua, Mexico with the goal of validating the prototype and gathering patient samples . Data produced in patient trials was reviewed and analyzed with the goal of determining typical values out of the healthy and injured groups. Statistical metrics were computed to compare results among groups. Later on, some of these metrics were implemented as classification parameters. Overall error rate was calculated for each of the different tries. Restricting the use of only X and Z axis data, backed up in the idea that X reports the internal tibial rotation, and Z takes care of the anterior-posterior tibial translation with respect of the femur, became the approach leading to the minimum error rate. Optimal results out of these classifiers had an average error rate of 30% approximately for both left and right legs.

After performing these tests and with the intention of implementing a non parametric classification method, pattern recognition k nearest neighbors algorithm was used as classification rule. Reported results coming from this approach proved to be

more effective reaching 25% and 15% error rates for left and right legs respectively.

Data is a precious resource, and in a time period little over than a year data results from over 150 patients were collected. Getting data of injured patients proved to be challenging but still possible. Nevertheless, given the results and the fact that those were purely based on acceleration readings from the very first prototype, grows the curiosity of seeing how the addition of rotational data (from the gyroscopes) can or cannot add more significant features towards improving the classification results of future patient trials.

Appendix A

Arduino and Processing Code

Code repository:

`https://maespinozas@bitbucket.org/maespinozas/pivotshift.git`

References

[1] V. Duthon, C. Barea, S. Abrassart, J. Fasel, D. Fritschy, and J. Ménétrey, "Anatomy of the anterior cruciate ligament," *Knee surgery, sports traumatology, arthroscopy*, vol. 14, no. 3, pp. 204–213, 2006. [Online]. Available: http://link.springer.com/article/10.1007/s00167-005-0679-9

[2] J. H. Mink, T. Levy, and J. Crues 3rd, "Tears of the anterior cruciate ligament and menisci of the knee: MR imaging evaluation." *Radiology*, vol. 167, no. 3, pp. 769–774, 1988. [Online]. Available: http://pubs.rsna.org/doi/abs/10.1148/radiology.167.3.3363138

[3] W. H. A. Ng, J. F. Griffith, E. H. Y. Hung, B. Paunipagar, B. K. Y. Law, and P. S. H. Yung, "Imaging of the anterior cruciate ligament," *World journal of orthopedics*, vol. 2, no. 8, p. 75, 2011. [Online]. Available: http://www.ncbi.nlm.nih.gov/pmc/articles/PMC3302044/

[4] S. Arneja and J. Leith, "Review article: Validity of the KT-1000 knee ligament arthrometer," *Journal of Orthopaedic Surgery*, vol. 17, no. 1, 2009. [Online]. Available: http://www.josonline.org/index.php/JOS/article/view/432;http://www.josonline.org/index.php/JOS/article/view/432/375

[5] S. Wiertsema, H. Van Hooff, L. Migchelsen, and M. Steultjens, "Reliability of the KT1000 arthrometer and the Lachman test in patients with an ACL rupture," *The Knee*, vol. 15, no. 2, pp. 107–110, 2008. [Online]. Available: http://www.sciencedirect.com/science/article/pii/S0968016008000082

[6] M.-H. Lam, D. T. Fong, P. S. Yung, E. P. Ho, W.-Y. Chan, and K.-M. Chan, "Knee stability assessment on anterior cruciate ligament injury: Clinical and biomechanical approaches," *BMC Sports Science, Medicine and Rehabilitation*, vol. 1, no. 1, p. 20, 2009. [Online]. Available: http://www.biomedcentral.com/1758-2555/1/20/

[7] P. H. Araujo, M. Ahlden, Y. Hoshino, B. Muller, G. Moloney, F. H. Fu, and V. Musahl, "Comparison of three non-invasive quantitative measurement systems for the pivot shift test," *Knee Surgery, Sports Traumatology, Arthroscopy*, vol. 20, no. 4, pp. 692–697, 2012. [Online]. Available: http://link.springer.com/article/10.1007/s00167-011-1862-9;http://link.springer.com/article/10.1007/s00167-011-1862-9/fulltext.html

[8] F. R. Noyes, E. S. Grood, J. F. Cummings, and R. R. Wroble, "An analysis of the pivot shift phenomenon The knee motions and subluxations induced by different examiners," *The American journal of sports medicine*, vol. 19, no. 2, pp. 148–155, 1991. [Online]. Available: http://ajs.sagepub.com/content/19/2/148.short

[9] V. Musahl, A. D. Pearle, and R. F. Warren, "Measurement Validation of Navigation During the Pivot-Shift Test," *Operative Techniques in Orthopaedics*, vol. 18, no. 3, pp. 181–184, 2008. [Online]. Available: http://www.sciencedirect.com/science/article/pii/S1048666609000044

[10] C. Reas and B. Fry, *Getting Started with Processing.* " O'Reilly Media, Inc.", 2010.

[11] *Official I2C Specification*, NXP Semiconductors. [Online]. Available: http://www.nxp.com/documents/user_manual/UM10204.pdf

[12] M. Banzi, *Getting Started with arduino.* " O'Reilly Media, Inc.", 2009.

[13] *Wiring: an open-source programming framework for microcontrollers* , Hernando Barragan. [Online]. Available: http://wiring.org.co/

[14] *ATmega48A/PA/88A/PA/168A/PA/328/P Summary*, Atmel. [Online]. Available: www.atmel.com/images/doc8161.pdf

[15] J. L. Hennessy and D. A. Patterson, *Computer Architecture - A Quantitative Approach (5. ed.).* Morgan Kaufmann, 2012.

[16] A. J. Wixted, D. V. Thiel, A. G. Hahn, C. J. Gore, D. B. Pyne, and D. A. James, "Measurement of energy expenditure in elite athletes using MEMS-based triaxial accelerometers," *Sensors Journal, IEEE*, vol. 7, no. 4, pp. 481–488, 2007. [Online]. Available: http://ieeexplore.ieee.org/xpls/abs_all.jsp?arnumber=4105926

[17] T.-R. Hsu, *MEMS & microsystems: design, manufacture, and nanoscale engineering.* John Wiley & Sons, 2008.

[18] B. Evans, *Beginning Arduino Programming*. Apress, 2011.

[19] D. Ibrahim, *Advanced PIC microcontroller projects in C: from USB to RTOS with the PIC 18F series*. Newnes, 2011.

[20] *Adafruit_LSM9DS0_Library* , Adafruit. [Online]. Available: https://github.com/adafruit/Adafruit_LSM9DS0_Library

[21] *GNU Lesser General Public License* , The Free Software Foundation. [Online]. Available: https://www.gnu.org/licenses/lgpl.html

[22] C. Reas and B. Fry, *Processing: a programming handbook for visual designers and artists*. Mit Press, 2007.

[23] *controlP5: A GUI (graphical user interface) library for processing* , Andreas Schlegel. [Online]. Available: http://www.sojamo.de/libraries/controlP5/

[24] M. Summerfield, *Rapid GUI Programming with Python and Qt : the Definitive Guide to PyQt Programming*, 2007.

[25] *matplotlib: python plotting library* , John Hunter. [Online]. Available: http://matplotlib.org/

[26] *NumPy library* , Scipy.org. [Online]. Available: http://www.numpy.org/

[27] *psych: Procedures for Psychological, Psychometric, and Personality Research* , William Revelle. [Online]. Available: http://cran.r-project.org/web/packages/psych/index.html

[28] L. A. Kelly, D. G. McMillan, A. Anderson, M. Fippinger, G. Fillerup, and J. Rider, "Validity of actigraphs uniaxial and triaxial accelerometers for assessment of physical activity in adults in laboratory conditions," *BMC medical physics*, vol. 13, no. 1, p. 5, 2013.

[29] L. Engebretsen, C. A. Wijdicks, C. J. Anderson, B. Westerhaus, and R. F. LaPrade, "Evaluation of a simulated pivot shift test: a biomechanical study," *Knee Surgery, Sports Traumatology, Arthroscopy*, vol. 20, no. 4, pp. 698–702, 2012. [Online]. Available: http://link.springer.com/article/10.1007/s00167-011-1744-1;http://link.springer.com/article/10.1007/s00167-011-1744-1/fulltext.html

[30] R. O. Duda, D. G. Stork, and P. E. Hart, *Pattern classification*. New York; Chichester: Wiley, 2000.

[31] R. Faludi, *Building wireless sensor networks: with ZigBee, XBee, arduino, and processing.* " O'Reilly Media, Inc.", 2010.

[32] N. Lopomo, S. Zaffagnini, S. Bignozzi, A. Visani, and M. Marcacci, "Pivot-shift test: Analysis and quantification of knee laxity parameters using a navigation system," *Journal of Orthopaedic Research*, no. 2, pp. 164–169, 2010.